

Investigations on a Portion of the Quaternary System $\text{CaO-Al}_2\text{O}_3\text{-SiO}_2\text{-Fe}_2\text{O}_3$: The Quaternary System $\text{CaO-2CaO.SiO}_2\text{-5CaO.3Al}_2\text{O}_3\text{-4CaO.Al}_2\text{O}_3\text{-Fe}_2\text{O}_3$

F. M. Lea and T. W. Parker

Phil. Trans. R. Soc. Lond. A 1934 **234**, 1-41

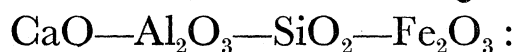
doi: 10.1098/rsta.1934.0023

Email alerting service

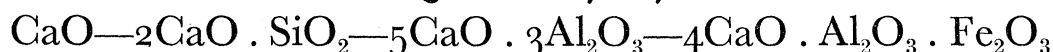
Receive free email alerts when new articles cite this article - sign up in the box at the top right-hand corner of the article or click [here](#)

To subscribe to *Phil. Trans. R. Soc. Lond. A* go to: <http://rsta.royalsocietypublishing.org/subscriptions>

I—Investigations on a Portion of the Quaternary System



The Quaternary System



By F. M. LEA and T. W. PARKER.

(Communicated by Sir FRANK SMITH, Sec. R.S. Received April 20—Read June 24, 1934)

[PLATE 1]

INTRODUCTION

The quaternary system investigated in the present work is of considerable interest from both scientific and technical points of view. In particular, the phase relationships in that part of the system having a high lime and low iron content are of fundamental importance in the study of Portland cement. It was with the object of elucidating these phase relationships in the study of Portland cement that this investigation was undertaken, but it was necessary to examine the system much beyond the limits of cement compositions. The results have perhaps a particular interest as representing the working out of a complete polythermal condensed quaternary system. Apart from certain limited studies on metals, we are not aware of any such complete system having previously been reported in the literature.

THEORETICAL

In the investigation of a ternary system, it is desirable to have data for the three binary systems which make up the sides of the triangle in which the ternary compositions are plotted, before exploring the interior. Similarly, for a quaternary system, it is desirable first to have data for four ternary systems before determining data for points containing all four components. In the major system $\text{CaO—Al}_2\text{O}_3\text{—SiO}_2\text{—Fe}_2\text{O}_3$, some of the ternary systems have already been worked out. RANKIN and WRIGHT* give complete data for the system $\text{CaO—Al}_2\text{O}_3\text{—SiO}_2$; HANSEN, BROWNMILLER and BOGUE† have outlined part of the system $\text{CaO—Al}_2\text{O}_3\text{—Fe}_2\text{O}_3$ and HANSEN and BOGUE‡, the products of final crystallization in the high lime portion of the system $\text{CaO—SiO}_2\text{—Fe}_2\text{O}_3$. No data are available on the system $\text{Al}_2\text{O}_3\text{—SiO}_2\text{—Fe}_2\text{O}_3$, but it is not to be expected that phases present in this

* 'Amer. J. Sci.,' vol. 34, p. 1 (1915).

† 'J. Amer. Chem. Soc.,' vol. 50, p. 396 (1928).

‡ 'J. Amer. Chem. Soc.,' vol. 48, p. 1261 (1926).

system will influence the quaternary system explored in the present work and the system of the three acidic oxides can therefore be neglected.

From the data of RANKIN and WRIGHT, it is shown that the three compounds CaO , $2\text{CaO} \cdot \text{SiO}_2$ and $5\text{CaO} \cdot 3\text{Al}_2\text{O}_3$ form a true ternary system within the larger system $\text{CaO}-\text{Al}_2\text{O}_3-\text{SiO}_2$. Similarly, inspection of the system $\text{CaO}-\text{Al}_2\text{O}_3-\text{Fe}_2\text{O}_3$ shows that a true ternary system is formed by the compounds CaO , $4\text{CaO} \cdot \text{Al}_2\text{O}_3 \cdot \text{Fe}_2\text{O}_3$ and $5\text{CaO} \cdot 3\text{Al}_2\text{O}_3$. Since HANSEN and BOGUE have also shown that no ternary compounds are to be expected in the system $\text{CaO}-\text{SiO}_2-\text{Fe}_2\text{O}_3$, it seemed probable that a true quaternary system might be formed by the four compounds $\text{CaO}-2\text{CaO} \cdot \text{SiO}_2-5\text{CaO} \cdot 3\text{Al}_2\text{O}_3-4\text{CaO} \cdot \text{Al}_2\text{O}_3 \cdot \text{Fe}_2\text{O}_3$. The present investigation has shown this to be so and work has therefore been confined to this system, which has been completely determined. Since the previous literature on the subject has rendered it more familiar, results as presented later are sometimes shown in the form of the larger system $\text{CaO}-\text{Al}_2\text{O}_3-\text{SiO}_2-\text{Fe}_2\text{O}_3$.

Graphical methods for the representation of systems of four components involve the use of a space model in the form of a tetrahedron. An isotherm of a condensed* quaternary system may be completely defined in a diagram plotted in this way, but where temperature is also a variable, it is necessary to adopt some device to condense the data on to one model. The simplest method is essentially an extension of that normally used for three component polythermal systems, which consists in plotting a series of fields, in each of which one compound is the primary phase, *i.e.*, the phase which, on cooling the liquid, is the first to crystallize. Temperature isotherms in the fields are obtained by connecting up points of the same final melting temperature. The extension of the method to a tetrahedral diagram of four components again produces a series of fields for the primary phases, but the fields are now volumes instead of areas. Between two adjacent fields, or volumes, there exists a boundary surface, in which two solid phases coexist with liquid and vapour. The line along which three such boundary surfaces intersect represents the points of contact of three primary phase volumes and corresponds to compositions having three solid phases in equilibrium with liquid and vapour. They are referred to as quintuple lines. Finally, the invariant, or sextuple, point where four primary phase volumes and four boundary surfaces meet, represents the composition where four solid phases are in equilibrium with liquid and vapour. An invariant point may or may not be a eutectic, depending on the temperature distribution along the quintuple lines leading to it. Isotherms introduced into a diagram of this type now take the form of surfaces, the isothermal lines in the ternary systems bounding the quaternary system representing the intersection of the isothermal surfaces with the bounding ternary system planes. Except in very simple examples, however, the

* While the present system can be treated as condensed, it is convenient in applying terminology to count the vapour phase. A quaternary eutectic is thus termed a sextuple point counting four solid phases, liquid and vapour. Though seemingly inconsistent, it is necessary to do this to avoid confusion, since it was the convention followed by RANKIN and WRIGHT in their classical paper on the ternary system $\text{CaO}-\text{Al}_2\text{O}_3-\text{SiO}_2$ (*loc. cit.*) and has since been adopted by other workers. In the discussion an actual mention of the vapour phase is often omitted.

QUATERNARY SYSTEM $\text{CaO—Al}_2\text{O}_3\text{—SiO}_2\text{—Fe}_2\text{O}_3$

3

introduction of all the data on to one diagram causes much complexity. It is frequently sufficient merely to indicate the direction of falling temperature along the quintuple lines by means of arrows. The main advantage of the insertion of the isothermal surfaces into the tetrahedron is that from such a diagram any isotherm may be directly obtained.

The temperature relations in quaternary systems, which have been discussed by BOCKE* from graphical considerations, may be derived by an extension of the deductions of GIBBS† relating to binary and ternary systems.

For a condensed system GIBBS' well-known equation (97) relating to the conditions of equilibrium in a phase reduces to

$$-\eta dt = m_1 d\mu_1 + m_2 d\mu_2 + \dots + m_n d\mu_n,$$

where η and t represent respectively the entropy and temperature, m_1, m_2, \dots, m_n the masses of the n components, and $\mu_1, \mu_2, \dots, \mu_n$ the chemical potentials of these components.

An equation of this type may be written down for each existing phase :—

$$-\eta' dt = m'_1 d\mu_1 + m'_2 d\mu_2 + \dots$$

$$-\eta'' dt = m''_1 d\mu_1 + m''_2 d\mu_2 + \dots$$

$$-\eta''' dt = m'''_1 d\mu_1 + m'''_2 d\mu_2 + \dots$$

The condition of equilibrium between these phases is that t, μ_1, μ_2 etc., have the same value throughout. Applying this condition to a series of these equations, one for each phase present, the necessary relations between the ratios of the different masses in the various phases such that the temperature may be a maximum or minimum ($dt = 0$) can be deduced. GIBBS considers in this way certain binary and ternary systems and a simple extension of his method to quaternary systems leads to the various general temperature relationships.

For example, along a quintuple line‡ in a condensed quaternary system three solid phases and a liquid coexist in equilibrium. The four phase equations are :—

$$\text{Solid A} \quad -\eta' dt = m'_1 d\mu_1 + m'_2 d\mu_2 + m'_3 d\mu_3 + m'_4 d\mu_4$$

$$\text{Solid B} \quad -\eta'' dt = m''_1 d\mu_1 + m''_2 d\mu_2 + m''_3 d\mu_3 + m''_4 d\mu_4$$

$$\text{Solid C} \quad -\eta''' dt = m'''_1 d\mu_1 + m'''_2 d\mu_2 + m'''_3 d\mu_3 + m'''_4 d\mu_4$$

$$\text{Liquid} \quad -\eta'''' dt = m''''_1 d\mu_1 + m''''_2 d\mu_2 + m''''_3 d\mu_3 + m''''_4 d\mu_4.$$

* 'Z. anorg. Chem.,' vol. 98, p. 203 (1916).

† "Collected Works of Willard Gibbs," vol. 1, p. 100.

‡ This case is a special one of the general case of n components and n phases for which SCHREINEMAKER (Roozeboom, 'Die Heterogenen Gleichgewichte,' vol. 3, part 1, p. 285; 'Proc. Acad. Sci. Amst.,' vol. 19, p. 1205 (1917)) and MOREY and WILLIAMSON ('J. Amer. Chem. Soc.,' vol. 40, p. 58 (1918)) have deduced that the temperature is a maximum when a phase reaction is possible, i.e., when the composition of one of the n phases can be expressed in terms of the other $(n - 1)$, or fewer, phases.

Eliminating $d\mu_2$, $d\mu_3$ and $d\mu_4$ we get :—

$$d\mu_1 \begin{vmatrix} m'_1 & m'_2 & m'_3 & m'_4 \\ m''_1 & m''_2 & m''_3 & m''_4 \\ m'''_1 & m'''_2 & m'''_3 & m'''_4 \\ m''''_1 & m''''_2 & m''''_3 & m''''_4 \end{vmatrix} = dt \begin{vmatrix} -\eta' m'_2 m'_3 m'_4 \\ -\eta'' m''_2 m''_3 m''_4 \\ -\eta''' m'''_2 m'''_3 m'''_4 \\ -\eta'''' m''''_2 m''''_3 m''''_4 \end{vmatrix}$$

The condition for the coefficient of $d\mu_1$ to be zero, and hence for $dt = 0$ is :—

$$\begin{aligned} m''''_1 &= zm'_1 + xm''_1 + ym'''_1 \\ m''''_2 &= zm'_2 + xm''_2 + ym'''_2 \\ m''''_3 &= zm'_3 + xm''_3 + ym'''_3 \\ m''''_4 &= zm'_4 + xm''_4 + ym'''_4 \end{aligned}$$

The condition for a maximum or minimum in temperature ($dt = 0$) along a quintuple line is, therefore, that the composition of the liquid must be such that it can be made up of the three solid phases A, B and C which exist in equilibrium with it. The liquid composition must therefore lie in the plane containing the three solid phases. The identification of $dt = 0$ as a maximum follows from SCHREINERMAKER'S deductions (*loc. cit.*). The point where the quintuple line of solids A, B, C and liquid cuts the ternary conjugation plane A B C is a maximum on the quintuple line. It is also a point of minimum temperature (a ternary eutectic or an invariant point) in the ternary plane A B C.

The more useful temperature relationships which can be deduced by similar methods, considering also the boundary surfaces (2 solid and 1 liquid phases) and the primary phase volumes (1 solid and 1 liquid phase), are as follows :—

(1) In a quaternary system the melting point of any congruently melting compound will be a temperature maximum in its own primary phase volume. If it melts incongruently to give a liquid and another solid, its composition will fall outside its primary phase volume which then contains no temperature maximum. In this latter system temperatures rise in the primary phase volume towards the surface adjacent to the composition point of the compound concerned.

(2) The boundary surface between two primary phase volumes will show a temperature maximum where it is cut by the line joining the compositions of the two compounds concerned. The point of intersection is a minimum temperature on this conjugation line ; it is the binary eutectic of the two compounds which thus form a binary system within the quaternary system.* If the conjugation line does not cut the common boundary surface, temperatures will rise along the surface towards that edge which is adjacent to the conjugation line, but no temperature maximum occurs in the surface. The two compounds concerned do not now form

* This rule holds whether the compounds concerned melt congruently or not, but in the latter case only a partial, and not a complete, binary system is formed.

a binary system, the conjugation line lies partly in the primary volume of some third phase and the temperature relations along it have no special significance.

(3) As has been discussed in the example above, the quintuple line, along which the primary phase volumes of three compounds meet, possesses a temperature maximum where it intersects the conjugation plane of the three compounds; the point of intersection is the ternary eutectic or invariant point of the three compounds which form a ternary system within the quaternary. Where the point is an invariant, but not a eutectic, the three compounds form only a partial ternary system constituting part of a larger complete ternary system lying in the same plane. As an obvious corollary the temperature must fall along all quintuple lines which lead from one (ternary) face of a quaternary system into the interior volume. If the quintuple line does not intersect the conjugation plane it shows no temperature maximum, but the temperature rises along it in a direction towards that plane. The three compounds then do not form a ternary system.

(4) A sextuple point where four primary phase volumes meet, and at which four solid and one liquid phases coexist, will be a eutectic point if it falls within the volume bounded by the four conjugation planes made up by joining the solid phase compositions three at a time. If it falls outside this volume it is an invariant point, but not a eutectic.

(5) The plane of a ternary system within a quaternary system is one of maximum temperature across the tetrahedral model and temperatures fall away on either side of it. Similarly, the line of a binary system is a line of maximum temperatures across that portion of the tetrahedral model which it traverses. No crystallization path for any mix can cross a binary conjugation line or ternary conjugation plane of this type.

(6) The temperature relations in plane sections taken at random across the tetrahedron depend on the orientation of the plane and have no special significance. Such a plane may cut through several primary phase volumes and the lines of intersection of their bounding surfaces with the plane will form boundary lines to primary phase fields in the plane. Temperature maxima or minima may occur along such boundary lines or in such planes, but they also are without special significance.

The detailed application of the general rules to the various special cases arising in the present system will be taken up later. They form the basis for the interpretation of the temperature relations in the system, and are essential for deciding the direction of fall of temperature along certain boundary surfaces and quintuple lines where the actual temperature gradients are too slight to be ascertained experimentally. The present system shows little solid solution and the additional complexities introduced by the latter need not be considered.

The course of crystallization of compositions within the four component tetrahedron is somewhat more complicated than in the case of ternary systems. The latter have been discussed in detail by RANKIN and WRIGHT (*loc. cit.*) and this, together with a discussion of possible cases in quaternary systems by BOCKE (*loc. cit.*), affords a basis

on which certain general rules, which are of assistance in experimental work on such systems, may be developed. In cooling a liquid of any composition represented by a point in the tetrahedron, in the simplest course, the primary phase will first separate, while the composition of the residual liquid will change along the prolongation of a line connecting the original point and the composition point of the phase separating, and in a direction away from the latter point, until a boundary surface is reached. At this point, two phases separate and the course of the residual liquid is defined by the line formed by the intersection of the boundary surface with a plane containing the compositions of the two separating phases and the original mix. At any given temperature, the composition of the liquid on the boundary surface is represented by a point. A line joining this point and the original composition, prolonged backwards, must intersect the line joining the compositions of the two phases separating, and the point of intersection represents the mean composition of the solid which has separated down to the given temperature. The tangent plane to the boundary surface at the point representing the liquid composition must cut either the line joining the compositions of the two phases separating, or this line produced. The point of intersection represents the composition of the solid separating at that point on the boundary surface. When the intersection is with the composition line produced, one of the solid phases must be redissolving while the other is separating out. It may be shown that, when the re-resolution continues until one phase has completely disappeared, the prolongation of the line from the liquid composition point through the original mix composition point will now pass through the composition of the remaining separating phase. When this condition is reached, the liquid composition leaves the boundary surface on lowering the temperature, and continues through a primary phase volume.

The separation of three crystalline phases occurs when the liquid composition has traversed its defined path over the boundary surface and has reached a quintuple line. The path of the liquid is now along the quintuple line in the direction of falling temperature. The line through any given point traversed by the liquid composition on the quintuple line and the original composition, when produced, must intersect the triangular ternary plane whose apices are the compositions of the three separating phases; the point of intersection represents the mean composition of the solid which has separated. The tangent to the quintuple line at any point* must cut either this ternary plane or extensions of it, and the intersection represents the composition of the solid separating at that point. If re-resolution of one of the phases takes place and the phase completely disappears, the path of the liquid moves away from the quintuple line and crosses the boundary surface between the two residual phases until it again meets a quintuple line.

The liquid composition path along a quintuple line eventually reaches an invariant point which may be either a sextuple point or a quaternary eutectic. In the first case the crystallization curve may end with the separation of four solid phases, or

* This tangent lies in the same plane as that part of the quintuple line close to the point selected.

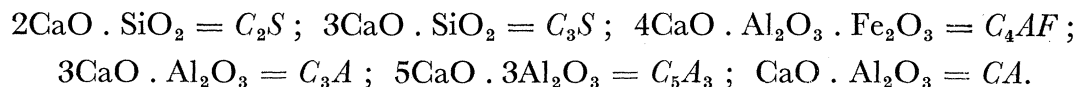
following similar considerations to those above, one solid phase may redissolve completely, the liquid path then continuing along another quintuple line.

These types of crystallization paths are encountered in the system $\text{CaO—2CaO . SiO}_2\text{—5CaO . 3Al}_2\text{O}_3\text{—4CaO . Al}_2\text{O}_3 . \text{Fe}_2\text{O}_3$ and are discussed later.

Methods

(1) *General*—For practical purposes, it is obviously necessary to devise some short cuts to the definition of the system. This may often be attempted by the solving of various binary and ternary systems which may exist within the quaternary. Indeed, by any method it is always of use to plot out these simpler systems, but it is necessary also to explore the quaternary regions proper. In the present investigation, this has been done by examining a series of what may be termed pseudo-ternary systems, each system containing a definite constant amount of ferric oxide. In other words, if ferric oxide is plotted at the apex of the tetrahedron, a series of planes parallel to the base have been examined.* It is then a simple operation to place them in their correct position in a tetrahedron and to estimate the boundary surfaces and lines from the reference data obtained. However, there are some limitations to the method. Experimentally, it is possible, for most compositions, to determine the temperature at which the first crystalline phase appears and also that at which the second, and in some cases, succeeding phases appear on cooling. In a ternary system therefore, one composition can give a considerable amount of data which can be readily plotted on to the diagram. When the method of pseudo-ternary planes in the quaternary system is used this is not generally possible, since the composition of the first solid phase to separate usually lies outside this plane and hence the crystallization path passes out of the plane as soon as primary crystals begin to appear. Generally, therefore, it is easier to investigate more points rather than to calculate them from the data on one point.

(2) *Experimental*—There has been developed a shorthand notation for the molecular compounds found in previous investigations.† This will be used in future reference to the compounds and the key is therefore given here :—



Materials used in this investigation were the purest products which could be purchased. Except for ferric oxide, they showed a satisfactory purity. The ferric

* An alternative method discussed theoretically by PARAVANNO ('Atti. R. Accad. Lincei,' vol. 20, ii, pp. 206, 331 (1911); 'Gazzetta,' vol. 42, ii, pp. 305, 589 (1912)) makes use of a series of planes through the composition point of the first solid to separate. It has both advantages and disadvantages compared with the present method.

† RANKIN and WRIGHT, 'Amer. J. Sci.,' vol. 34, p. 1 (1915); HANSEN, BROWNMILLER and BOGUE, 'J. Amer. Chem. Soc.,' vol. 50, p. 396 (1928); and HANSEN and BOGUE, *Ibid.*, vol. 48, p. 1261 (1926).

oxide used was first washed to remove soluble matter, the analysis of the final product is given in Table I. The impurities remaining consisted in the main of the other components, for which correction could be made in making up mixes.

TABLE I

	CaCO ₃		Al ₂ O ₃	SiO ₂	Fe ₂ O ₃	
	i	ii			i	ii*
CaO%	56.05	56.30	Nil	0.02	0.08	0.30
Al ₂ O ₃ %	Nil	0.046	99.762	0.093	0.06	0.12
SiO ₂ %	0.015	Nil	Trace	99.69	0.43	0.44
Fe ₂ O ₃ %	Nil	0.004	0.048	0.017	98.70	97.77
Ignition loss %	43.92	43.71	0.06	0.16	0.30	0.82
Na ₂ O%	0.013	0.03 (4)	0.05	Nil	0.25	0.12
K ₂ O%	Nil	0.00 (8)	0.02	Nil	Trace	0.07
MgO%	0.03	0.05	0.06	0.02	0.11	0.06
SO ₃ %	Nil	0.00 (2)	N.e. †	N.e.	0.07	0.06
Cl-%	Very slight trace	Nil	N.e.	N.e.	N.e.	N.e.
NO ₃ -%	Very slight trace	Nil	N.e.	N.e.	N.e.	N.e.
Mn ₃ O ₄ %	N.e.	N.e.	N.e.	N.e.	N.e.	0.24

Analyses by H. Andrews. * by W. G. Grindle. † N.e. = Not estimated.

In making up mixes, the calculated amounts of the raw materials were weighed into a dry bottle and shaken vigorously for some minutes. The mixture was then ground in an agate mortar to break up any lumpy material (since the ferric oxide tended to form small lumps) and reshaken. It is believed that the mix obtained in this way is as homogeneous as that obtained by wet mixing. All compositions were subsequently burned in muffle furnaces in platinum trays at 1200° C to decarbonate them and subsequently at higher temperatures up to 1500° C, the actual temperature depending on the composition of the mix and being such as to produce sintering. The last operation was repeated, the melt being ground through a 60-mesh sieve between the burns and finally, at the end of burning, through a 180-mesh sieve. Two muffle furnaces were used during the course of the investigation, one having Silit rods as the heating element, the other having platinum—20% rhodium alloy wire.

Temperature measurement in these and subsequent heat treatments was made by means of platinum—platinum 10% rhodium alloy thermocouples, the e.m.f. being measured by means of a potentiometer. Couples were initially standardized at the National Physical Laboratory and rechecked at the gold and palladium points in this laboratory before use. One couple was retained as a standard during the work and a chart for the deviation of this couple from the values given in ADAMS'

Tables* constructed from the two reference points at 1063°C (gold point), and 1554°C (palladium point), the deviation curve between the two points being represented as a straight line. These two reference points were periodically rechecked. It was observed with the couples in constant use that a very noticeable, progressive decrease in e.m.f. took place in all, when used between the temperatures of 1300 and 1600°C . It was therefore necessary constantly to calibrate the couples against the standard. The method adopted was to calibrate each couple after it had been in use for 60 hours and to apply a deviation correction to it. When the fall in e.m.f. had become too great or when the couple no longer gave constant values at any temperature, suitable amounts were cut from the wire at the hot junction and the end fused in an oxyhydrogen flame, the whole couple then being annealed at 1300°C . The calibration method was maintained without change throughout the work; the couple to be tested and the standard were maintained at 1450°C for one hour and the e.m.f.'s of both couples then taken at values of approximately 1450 , 1350 and 1200°C , constant temperature being maintained for at least 20 minutes before readings were taken at each temperature. Couples were calibrated in the quench furnaces, described later, and in the same position as that at which they were to be used.

For determination of phase equilibria, the quenching method was used. This method was developed by RANKIN and WRIGHT (*loc. cit.*) and for detailed accounts reference should be made to this and subsequent papers from the Geophysical Laboratory of the Carnegie Institute of Washington. A small charge, of the order of 0.05 gm from the mix under examination, wrapped in thin platinum foil, is suspended in the uniform temperature zone of a furnace and maintained at a known constant temperature until equilibrium is attained, a time of $\frac{3}{4}$ -1 hour being generally required in this particular investigation. At the end of the period, the charge is quenched rapidly by dropping it out of the furnace into a bath of water or mercury. If the temperature is such as to produce an unsaturated liquid in the charge, the resulting quenched charge is made entirely of glass, but if the temperature is such that the charge consists of liquid saturated with respect to any phase, the quenched charge contains glass and crystals. Determination of the condition of the quenched charge is made by powdering the specimen and examining under a petrographic microscope. By carrying out several experiments of this type at different temperatures, on a given mix, it is possible to obtain temperature limits at which the last crystalline phase finally goes into solution. In the present investigation, this method operated well, except in regions of low silica, high iron content, where, occasionally, crystallization during quenching took place to a certain extent. The apparatus used was also essentially the same as that developed by previous workers for silicate systems and involved the use of tube furnaces capable of being maintained at constant temperature to within $\mp 1^\circ$ even at the highest temperatures involved, 1650°C , over long periods of time; the Wheatstone Bridge method of control operating on the

* Int. Crit. Tables, vol. 1, p. 57 (1926).

furnace winding, with a primary relay operating a valve controlling the second and third stage relays, being used. Apart from minor modifications the control circuits were similar to those described by ROBERTS.* The furnaces were constructed of Norton Alundum tubes, 15" long, $\frac{7}{8}$ " inside diameter with a $\frac{1}{8}$ " wall, and wound over 7-8" with 0.8 mm diameter, platinum—20% rhodium alloy wire, 11 turns to the inch, beginning about $1\frac{1}{2}$ " from the bottom of the tube. Alundum tubes of $1\frac{5}{8}$ " bore, $\frac{1}{4}$ " wall, round the inner furnace tubes allowed of an air gap between the latter and the lagging material which was made up of a layer of magnesite $1\frac{1}{2}$ " thick, outside of which was a further 3" thickness of slag wool. The solid media of refractive index above 1.8 necessary for use in the immersion method for the examination of products under the microscope, were prepared after the manner given by LARSEN.†

The determination of invariant points was generally made by means of a heating curve. Checks on the quench results at other points were also carried out in this way. The most satisfactory method for use in the quenching furnaces, required about 1-2 gm of melt contained in a small platinum—3% rhodium alloy crucible, into which was sealed a septum, dividing the crucible into two separate portions. The crucible dimensions were :—height, 2.5 cm, diameter at top, 1.5 cm narrowing to a diameter of 1.0 cm at the bottom. Into one side of the crucible, fused alumina was filled as a "neutral" and a thermocouple plunged directly into the alumina. The other half held the melt to be tested, but the thermocouple was protected from the mix by covering it with a thin platinum sheath which was held rigidly in the centre of the melt by means of a small platinum spring. It was necessary to adopt this modification in order to avoid the sheath being dragged against the side after the first melting of the material. Thermocouples plunged directly into mixes containing iron oxides deteriorated very rapidly and the method of sheathing used here was necessary for this reason. A differential heating method was used, in which the temperature of the melt was read directly on one potentiometer and the difference in e.m.f. between the melt and the neutral couples on the other. For increasing the sensitivity, thermocouples of 0.2 mm diameter were occasionally used, but it was necessary to calibrate these much more frequently than the ordinary 0.5 mm couple. A Tinsley thermo-electric potentiometer, reading directly to 1 microvolt was used for measurement of the differential e.m.f. The rate of heating was 6° per minute with alternate readings at the minute and half minute respectively of the temperature of the melt and the differential while the furnace was advanced 3° at the quarter and three-quarter minute intervals. Fig. 1 shows typical graphs obtained from heating curves (*a*) being a curve with alumina in both sides of the septum and (*b*) a curve showing a thermal arrest at a sextuple point in the quaternary system.

* 'J. Opt. Soc. Amer. & Rev. Sci. Instr.,' vol. 11, p. 171 (1925).

† "Microscopic Determination of the Non-Opaque Minerals," 'U.S. Geol. Surv. Bull. No. 679,' Washington (1921), p. 16.

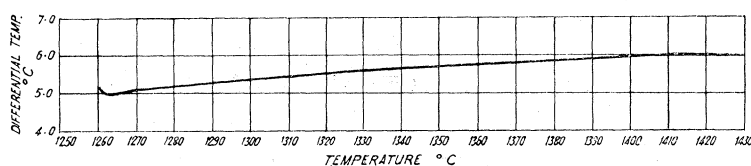
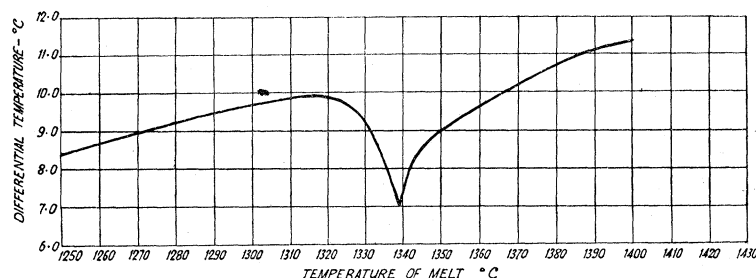


FIG. 1a—Heating curve with alumina in both sides of septum crucible.

FIG. 1b—Heating curve on F 103. Break at sextuple point $C_3S-C_2S-C_3A-C_4AF$. (1339° C.)

EXPERIMENTAL RESULTS

No new compounds were observed in the quaternary system or in the binary, and ternary systems investigated and the phases involved were, therefore, CaO , C_2S , C_3S , C_5A_3 and C_4AF . The boundary surface between the two high temperature forms of C_2S * was not sharply determined, but in that portion of the high alumina region where C_2S was the primary phase at temperatures below the $\alpha C_2S \rightarrow \beta C_2S$ inversion, the C_2S usually occurred as very small prismatic or tabular crystals, commonly of very simple outline. From the outline and faces observed, the symmetry would appear to be monoclinic; faces usually observed were the ortho- and clino-pinacoid pairs and the ortho- and clino-dome planes.

The refractive indices determined for C_3S were:— $\alpha = 1.718 \mp 0.003$, $\gamma = 1.724 \mp 0.003$. These are in close agreement with values obtained by other workers with this compound. The indices did not vary to any extent with changes in the iron content of melts from which they were crystallized. In melts of 20% Fe_2O_3 content the compound frequently occurred as small tabular crystals with well defined faces. Crystals were too small to determine the symmetry which may be trigonal, monoclinic or triclinic. †

The compounds containing alumina all entered into solid solution to a small extent. Thus, C_3A , C_5A_3 and CA appear to take up a small amount of iron oxide and thereby show a raising of refractive index. The highest index observed with C_3A was 1.723 ∓ 0.003 in a melt containing 16% Fe_2O_3 . C_5A_3 and CA were not examined in melts containing more than 10% Fe_2O_3 . In this, indices were:—for C_5A_3 , 1.621 ∓ 0.003 ; for CA , $\alpha = 1.654$, $\gamma = 1.670 \mp 0.003$. The indices of

* RANKIN and WRIGHT, *loc. cit.*† It has recently been shown (ANDERSEN and LEE, 'J. Wash. Acad. Sci.,' vol. 23, p. 338 (1933)) by measurements on large crystals of $3\text{CaO} \cdot \text{SiO}_2$, obtained from a basic open hearth slag, that this compound belongs to the trigonal system.

C_4AF appear to be lowered through slight solid solution with alumina, the lowest values observed being $\alpha_{Li} = 1.91$, $\gamma_{Li} = 1.96 \mp 0.02$. Refractive indices of the pure products determined by RANKIN and WRIGHT (*loc. cit.*) are :— C_3A , 1.710 ; C_5A_3 , 1.608 ; CA , $\alpha = 1.643$, $\gamma = 1.663$; C_4AF (HANSEN, BROWNMILLER and BOGUE (*loc. cit.*)) $\alpha_{Li} = 1.96$, $\gamma_{Li} = 2.04$.

With increasing iron content both C_3A and C_5A_3 tended to show better crystal development in quenches. In many of the melts in the 10% Fe_2O_3 pseudo system C_5A_3 occurred in small crystals apparently belonging to the tetrahedrite class of the cubic system, being frequently seen as crystals of triangular section and sometimes having facets corresponding in appearance to the three faced tetrahedron [$h k k$] (where $h > k$). C_3A occurred as grains showing hexagonal or octagonal outline with faces and edges not well defined. The development, however, was often sufficiently obvious to allow of its use in identifying the phase as an alternative method when the refractive index of the glass was close to that of C_3A and the identification of C_3A by means of its index had become difficult, as occurred with many melts in the 5 and 10% Fe_2O_3 pseudo-systems.

BINARY SYSTEMS

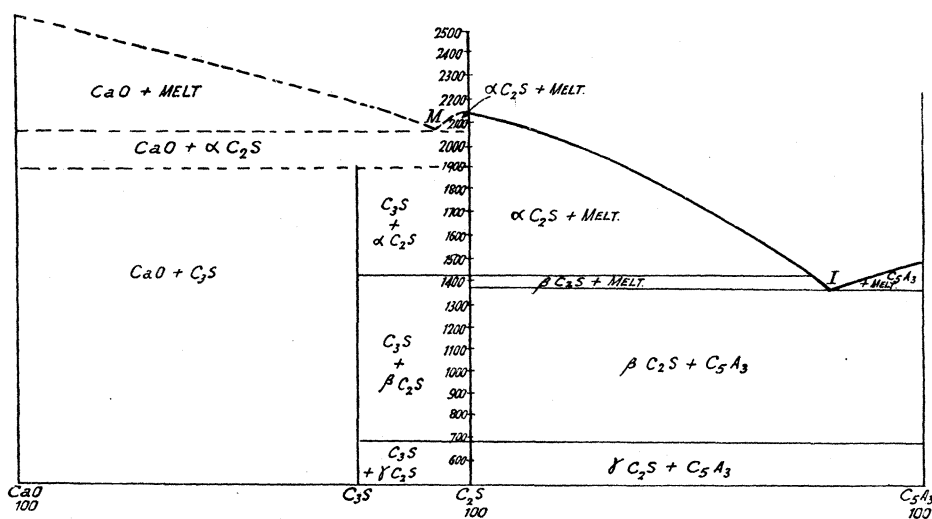
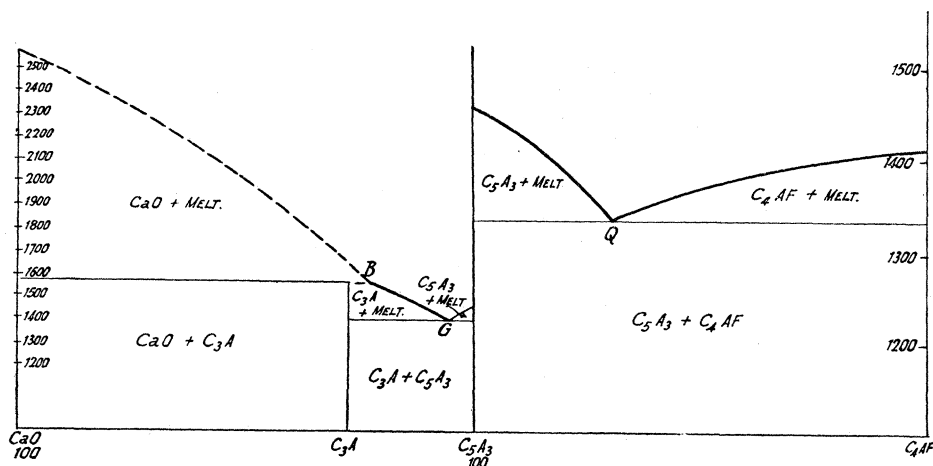
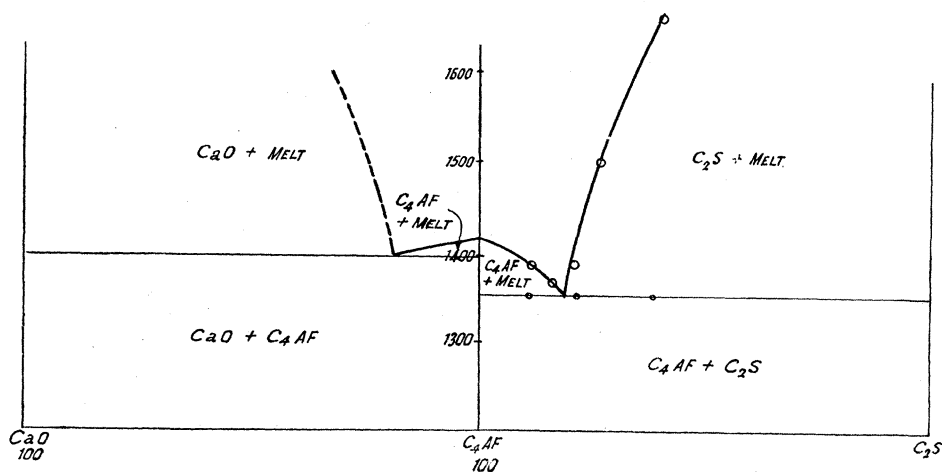
Of the six binary systems making up the edges of the tetrahedron in the system $CaO-C_2S-C_4AF-C_5A_3$, five are already known or can be derived from larger systems. These are shown in figs. 2 to 6. The remaining system is that of C_2S-C_4AF , on which no data were available. The results from the present investigation are shown in fig. 7 and the quench data from which it was obtained in Table II.

TABLE II—Mixes determining the System C_2S-C_4AF

Serial No.	Composition %		Quench data	Eutectic from heating curve
	CaO . Al_2O_3 . SiO_2 . Fe_2O_3	C_2S C_4AF		
F 129	48.0 : 18.9 : 3.5 : 29.6	10 90	{ 1390 All glass 1380 Glass + 4CaO . Al_2O_3 . Fe_2O_3 .	1353
F 128	48.9 : 17.8 : 5.2 : 28.0	15 85	{ 1380 All glass 1370 Glass + very rare 4CaO . Al_2O_3 . Fe_2O_3 .	
F 122	49.9 : 16.8 : 7.0 : 26.3	20 80	{ 1390 All glass 1380 Glass + occasional 2CaO . SiO_2 .	
F 175	51.1 : 15.7 : 8.7 : 24.7	25 75	{ 1500 Glass 1490 Glass + 2CaO . SiO_2	1358
F 123	53.7 : 12.6 : 14.0 : 19.7	40 60	1620 Glass + a little 2CaO . SiO_2	1345
F 125	55.6 : 10.5 : 17.5 : 16.5	50 50	1600 Glass + considerable 2CaO . SiO_2	
F 124	57.5 : 8.4 : 20.9 : 13.2	60 40	1600 Glass + considerable 2CaO . SiO_2	

QUATERNARY SYSTEM $\text{CaO}-\text{Al}_2\text{O}_3-\text{SiO}_2-\text{Fe}_2\text{O}_3$

13

FIG. 2—(A)—Concentration-Temperature Diagram of system $\text{CaO}-\text{C}_2\text{S}$.FIG. 3—(A)—System $\text{C}_2\text{S}-\text{C}_5\text{A}_3$.FIG. 4—(A)—System $\text{CaO}-\text{C}_6\text{A}_3$.FIG. 5—(B)—System $\text{C}_6\text{A}_3-\text{C}_4\text{AF}$.FIG. 6—(B)—System $\text{CaO}-\text{C}_4\text{AF}$.FIG. 7—(C)—System $\text{C}_2\text{S}-\text{C}_4\text{AF}$.

(A) Determination by RANKIN and WRIGHT.
 (C) Present investigation.

(B) HANSEN, BROWNMILLER and BOGUE.

The eutectic was determined from the compositions shown by means of heating curves. It may be seen that it is a simple system, the eutectic of C_4AF and C_2S occurring at a composition C_2S 18.5%, C_4AF 81.5% (CaO 49.6%, Al_2O_3 17.1%, SiO_2 6.5%, Fe_2O_3 26.8%) and a temperature of $1350 \pm 10^\circ C$.

TERNARY SYSTEMS

Two of the ternary systems already known (CaO— C_2S — C_5A_3 from RANKIN and WRIGHT (*loc. cit.*) and CaO— C_4AF — C_5A_3 from HANSEN, BROWNMILLER and BOGUE (*loc. cit.*)) are shown in their recalculated forms in figs. 8 and 9.

THE TERNARY SYSTEM CaO— C_2S — C_4AF

This system occurs as a plane through the larger system CaO— Al_2O_3 — SiO_2 . Fe_2O_3 . As far as the temperature limits permit of its experimental determination, it appears to be a true ternary system and as such is shown in figs. 10 and 10a with the data from which it was obtained in Table III. The boundary lines in fig. 10a relating to temperatures of final melting above $1600^\circ C$, were not determined experimentally since this was outside the limits of the furnace equipment. The form of the graph is rather similar to that of the system CaO— C_2S — C_5A_3 except that the C_3S field does not narrow with increasing lime content but, in the regions examined, shows the reverse behaviour. The extrapolation of the boundary

TABLE III—Data Determining the Ternary System CaO— C_2S — C_4AF

Serial No.	Composition %				Composition			Temperature	Quench data observed
	CaO	Al_2O_3	SiO_2	Fe_2O_3	CaO	C_4AF	C_2S		
F 184	55.25	14.69	6.96	23.08	10	70	20	{ 1460 Glass + traces of CaO { 1400 Glass + CaO + 3CaO . SiO_2 { 1460 Glass + CaO { 1400 Glass + CaO + 3CaO . SiO_2	
F 185	54.71	15.35	5.96	24.01	10	73	17	{ 1350 Glass + CaO + 3CaO . SiO_2 { 1340 Glass + CaO + 3CaO . SiO_2 + 4CaO . Al_2O_3 . Fe_2O_3	
F 196	53.66	16.48	4.03	25.83	10	78.5	11.5	{ 1380 Glass { 1370 Glass + CaO { 1360 Glass + CaO { 1350 Glass + CaO + 4CaO . Al_2O_3 . Fe_2O_3	
F 197	54.37	16.48	3.33	25.83	12	78.5	9.5	{ 1380 Glass + CaO { 1370 Glass + CaO + 4CaO . Al_2O_3 . Fe_2O_3	
F 198	55.07	16.48	2.63	25.83	14	78.5	7.5	{ 1390 Glass + CaO { 1380 Glass + CaO + 4CaO . Al_2O_3 . Fe_2O_3	
F 201	58.41	12.81	8.71	20.07	14	61	25	1600 Glass + CaO	
F 202	58.05	12.81	9.07	20.07	13	61	26	1600 Glass + CaO	

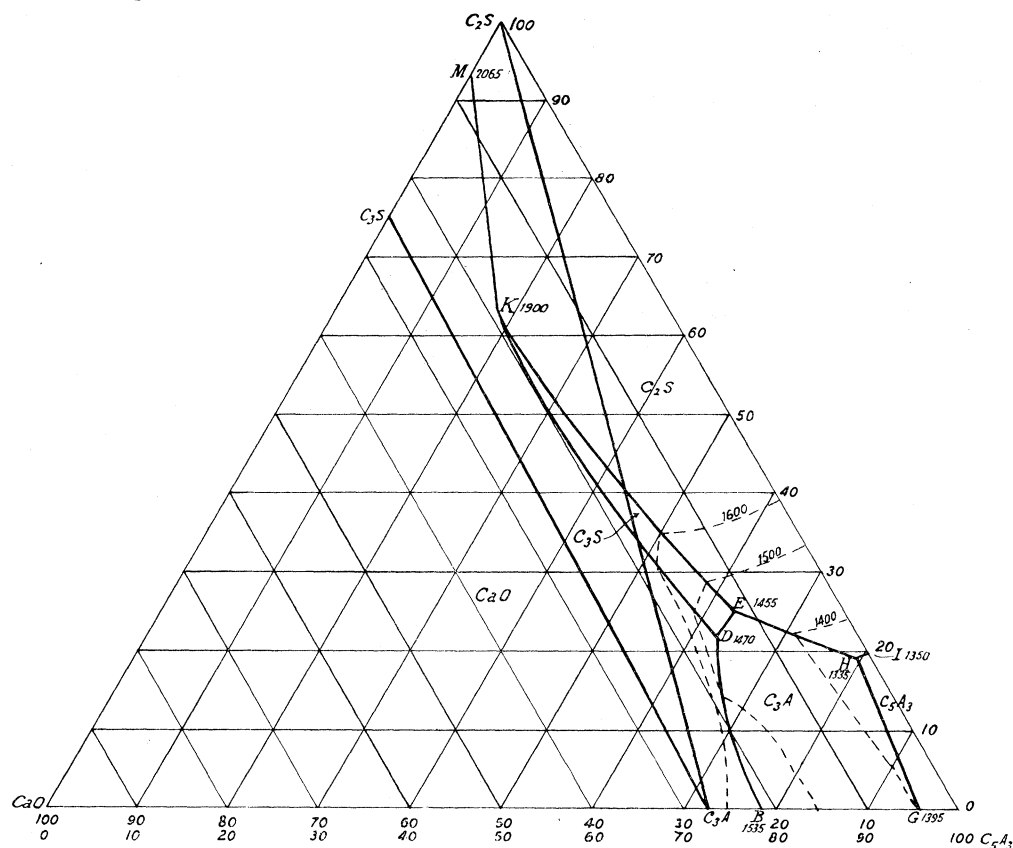


FIG. 8—System $\text{CaO}-\text{C}_2\text{S}-\text{C}_5\text{A}_3$. From RANKIN and WRIGHT. Showing isotherms to 1600°C .

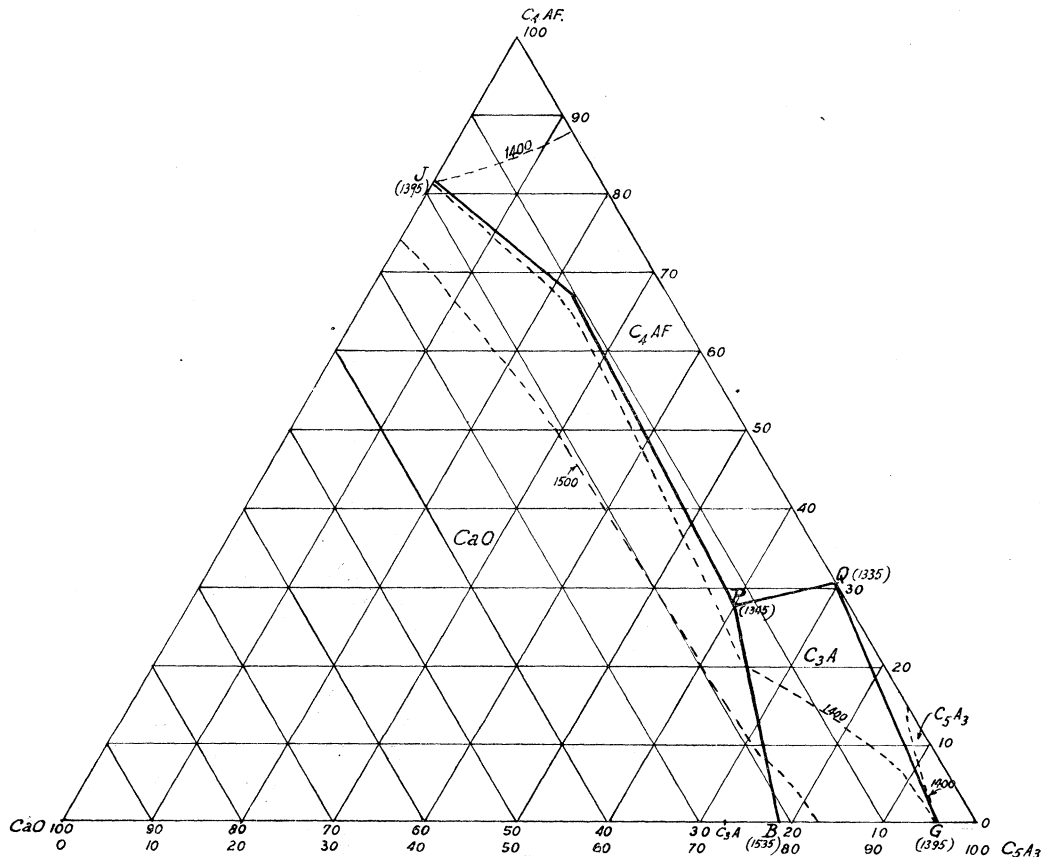


FIG. 9—System $\text{CaO}-\text{C}_4\text{AF}-\text{C}_5\text{A}_3$. From HANSEN, BROWNMILLER and BOGUE. Showing the probable course of isotherms at 1400°C and 1500°C .

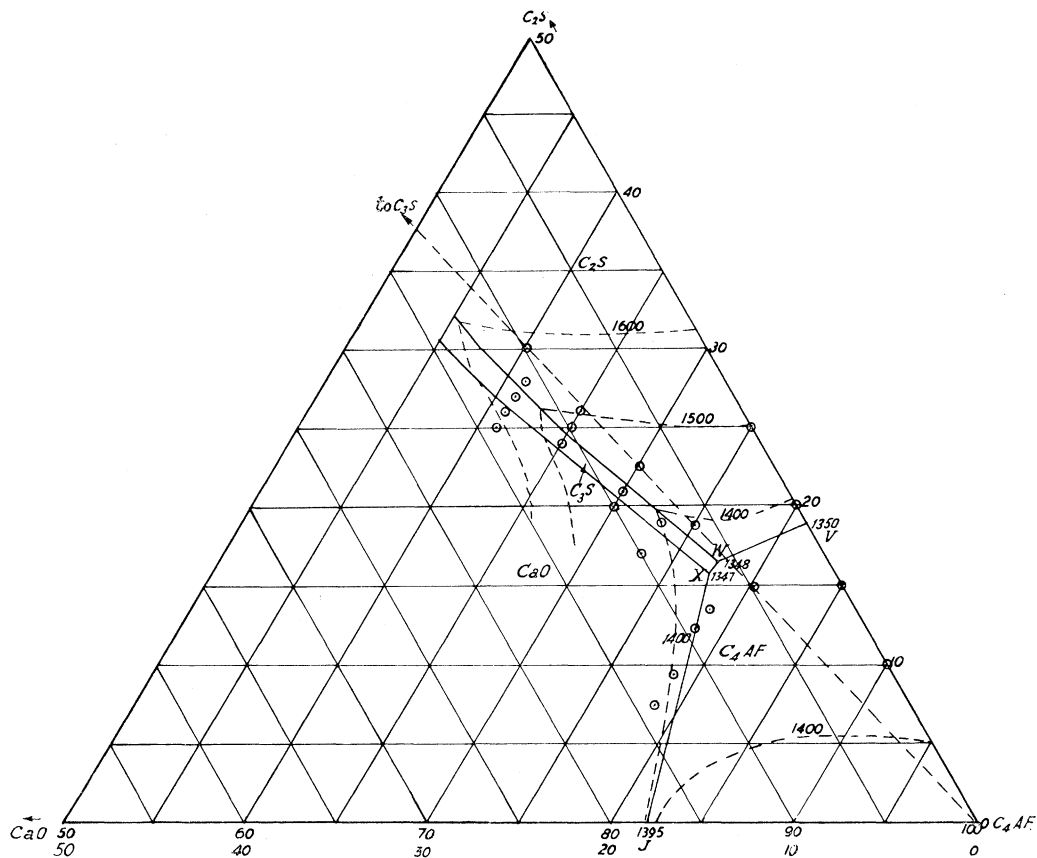


FIG. 10—System $\text{CaO}-\text{C}_2\text{S}-\text{C}_4\text{AF}$. Showing portion investigated. \circ = Experimental points.

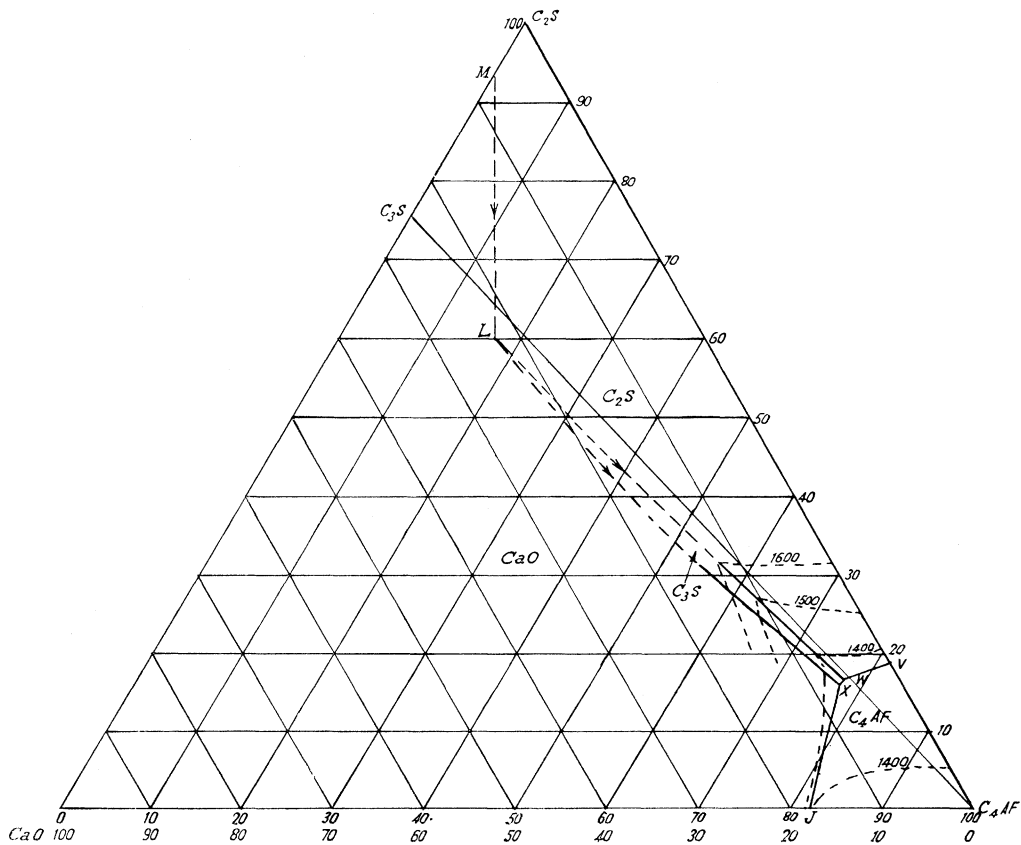


FIG. 10a—Ternary system $\text{CaO}-\text{C}_2\text{S}-\text{C}_4\text{AF}$. (Extrapolated boundary lines — — — —).

QUATERNARY SYSTEM $\text{CaO}-\text{Al}_2\text{O}_3-\text{SiO}_2-\text{Fe}_2\text{O}_3$

17

TABLE III—(continued)

Serial No.	Composition %				Composition			Temperature	Quench data Observed
	CaO	Al_2O_3	SiO_2	Fe_2O_3	CaO	C_4AF	C_2S		
F 203	57.71	12.81	9.41	20.07	12	61	27	{ 1600 Glass 1580 Glass + $3\text{CaO} \cdot \text{SiO}_2$	
F 204	57.35	12.81	9.77	20.07	11	61	28	{ 1560 Glass 1550 Glass + $3\text{CaO} \cdot \text{SiO}_2 + 2\text{CaO} \cdot \text{SiO}_2$	
F 186	54.93	14.69	7.30	23.08	9	70	21	{ 1450 Glass 1430 Glass + $3\text{CaO} \cdot \text{SiO}_2$	
F 187	54.03	15.35	6.61	24.01	8	73	19	{ 1410 Glass 1400 Glass + $3\text{CaO} \cdot \text{SiO}_2$	
F 188	56.59	13.63	8.36	21.40	11	65	24	{ 1480 Glass 1470 Glass + $3\text{CaO} \cdot \text{SiO}_2$	
F 189	56.25	13.63	8.71	21.40	10	65	25	{ 1510 Glass 1500 Glass + $2\text{CaO} \cdot \text{SiO}_2$	
F 190	55.88	13.63	9.06	21.40	9	65	26	{ 1490 Glass 1480 Glass + $2\text{CaO} \cdot \text{SiO}_2$	
F 117 (α)	54.37	14.69	7.90	23.04	7.38	70	22.6	{ 1480 Glass 1470 Glass + $2\text{CaO} \cdot \text{SiO}_2$	
F 118 (β)	57.13	12.60	10.53	19.75	(30 C_3S : 70 C_4AF)			{ 1600 Glass 1560 Glass + $2\text{CaO} \cdot \text{SiO}_2$	
					(40 C_3S : 60 C_4AF)				
F 176 (γ)	52.97	15.73	6.58	24.69	6.1	75	18.9	{ 1420 Glass	
								{ 1410 Glass + $2\text{CaO} \cdot \text{SiO}_2$	
								{ 1350 Glass + $2\text{CaO} \cdot \text{SiO}_2$ 1340 Glass + $2\text{CaO} \cdot \text{SiO}_2 + 4\text{CaO} \cdot \text{Al}_2\text{O}_3 \cdot \text{Fe}_2\text{O}_3$	
F 195	52.96	16.48	4.73	25.83	8	78.5	13.5	{ 1380 Glass	
								{ 1370 Glass + $4\text{CaO} \cdot \text{Al}_2\text{O}_3 \cdot \text{Fe}_2\text{O}_3$	
F 116 (δ)	51.60	16.79	5.26	26.34	4.9	80	15.1	{ 1380 Glass	
								{ 1370 Glass + $4\text{CaO} \cdot \text{Al}_2\text{O}_3 \cdot \text{Fe}_2\text{O}_3$	

(Mixes marked α , β , γ and δ are on the composition line of $C_3S - C_4AF$).

lines between C_3S —CaO and C_3S — C_2S is therefore much less certain. It should also be noted that in this system, the C_3S field lies entirely on the lime side of the C_4AF — C_3S line whereas, in the system CaO — C_2S — C_5A_3 , the field is entirely on the C_2S side of the C_3A — C_3S line. The difference involves changes in the type of crystallization curve in the C_3S field and surrounding regions of the diagram. Inspection of the diagram also shows that no true binary system is formed by the system C_4AF — C_3S . In part this is to be anticipated since RANKIN and WRIGHT have shown that the compound C_3S dissociates below its melting point to form CaO and C_2S . However, there was a possibility that the remainder of the system from the decomposition point might have been regarded as a true binary, but it may be seen that the primary phase crystallizing is either C_2S or C_4AF and that the C_3S —

C_4AF composition line does not cut the boundary between their fields. Fig. 11 shows points on this line plotted as for a binary system, but the diagram is not to be interpreted as a binary one. The small area containing $C_4AF + C_2S + \text{liquid}$ to the right of the invariant point is shown somewhat exaggerated in respect of the temperature interval.

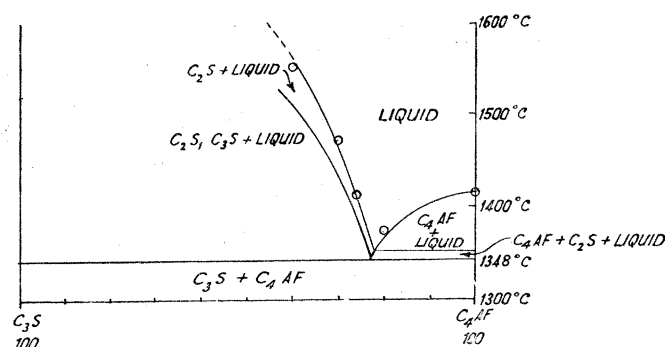


FIG. 11—Fusion temperatures and solid phase equilibria in mixes of C_3S and C_4AF .

The quintuple point at which CaO , C_3S and C_4AF are in equilibrium with liquid and vapour (point X, fig. 10a) occurs at a composition CaO 6.8%, C_2S 16%, C_4AF 77.2% (or CaO 52.8%, Al_2O_3 16.2%, SiO_2 5.6%, Fe_2O_3 25.4%), while the invariant point for the equilibrium of C_3S , C_2S and C_4AF with liquid and vapour (point W) is at CaO 6.0%, C_2S 16.5%, C_4AF 77.5% (or CaO 52.4%, Al_2O_3 16.3%, SiO_2 5.8%, Fe_2O_3 25.5%). By quenching, the temperature of both these points lies between 1345 and 1350° C, while by heating curves, arrests were obtained in both cases at 1349° C. Consideration of courses of crystallization within this system shows that the $\text{CaO}-C_3S-C_4AF$ point must be the ternary eutectic, the other being a quintuple point but not a eutectic; since the eutectic must have the lower temperature the values 1347° C and 1348° C are given respectively.

THE TERNARY SYSTEM $C_2S-C_5A_3-C_4AF$

This is the remaining system required to define the sides of the tetrahedron and is shown in fig. 12 with the data from which the diagram was derived in Table IV. It is a simple eutectic system, but as fewer points have been used to determine it than any of the others, the accuracy of the boundary lines is probably rather lower. In the field of C_5A_3 , crystallization was very rapid and the method of quenching did not give very good results. Occasionally round the $C_5A_3-C_2S$ boundary, an inversion of β to γ C_2S took place in the quench. Where β C_2S was developed in this system, crystals were of the form mentioned previously. The ternary eutectic in this system (point R) is at C_5A_3 54%, C_4AF 30%, C_2S 16% (CaO 50.0%, Al_2O_3 34.5%, SiO_2 5.6%, Fe_2O_3 9.9%), at a temperature of $1280 \pm 5^\circ$ C by heating curves.

QUATERNARY SYSTEM $\text{CaO}-\text{Al}_2\text{O}_3-\text{SiO}_2-\text{Fe}_2\text{O}_3$

19

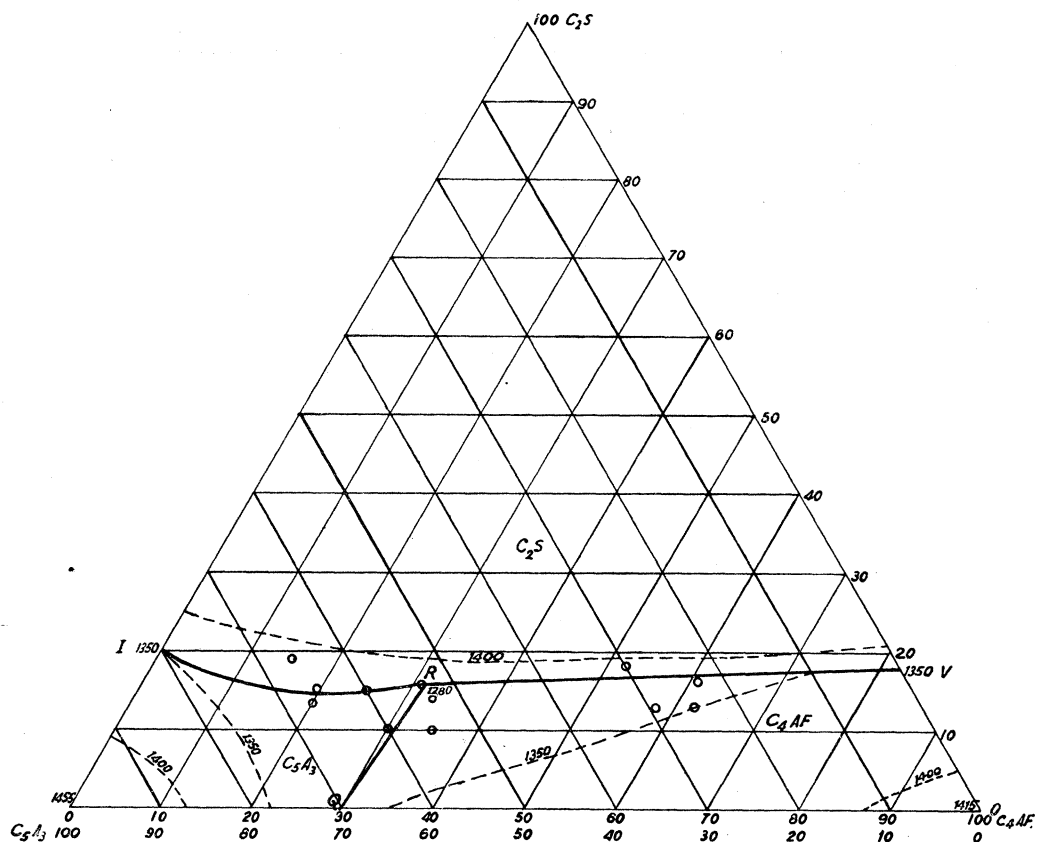


FIG. 12—System $C_2S-C_4AF-C_5A_3$ —Showing probable isotherms. \circ Points investigated.

TABLE IV—Data Determining the System $C_2S-C_5A_3-C_4AF$

Serial No.	Composition				Composition			Temperature	Quench data Observed
	CaO	Al_2O_3	SiO_2	Fe_2O_3	C_5A_3	C_4AF	C_2S		
F 181	49.10	27.28	4.53	19.09	29	58	13	1350 Glass 1340 Glass + $4\text{CaO} \cdot \text{Al}_2\text{O}_3 \cdot \text{Fe}_2\text{O}_3$	
F 183	49.03	26.05	4.53	20.39	25	62	13	1360 Glass 1350 Glass + $4\text{CaO} \cdot \text{Al}_2\text{O}_3 \cdot \text{Fe}_2\text{O}_3$ 1320 Glass	
F 192	48.97	36.00	3.48	11.53	55	35	10	1310 Glass + $4\text{CaO} \cdot \text{Al}_2\text{O}_3 \cdot \text{Fe}_2\text{O}_3$	
F 191	49.04	37.60	3.48	9.88	60	30	10	1310 Glass 1300 Glass + $5\text{CaO} \cdot 3\text{Al}_2\text{O}_3$	
F 200	49.67	35.54	4.89	9.89	56	30	14	1290 Glass 1285 Glass + rare $5\text{CaO} \cdot 3\text{Al}_2\text{O}_3$ + very rare $2\text{CaO} \cdot \text{SiO}_2$	
F 193	50.02	26.55	6.28	17.14	30	52	18	1340 Glass 1330 Glass + $2\text{CaO} \cdot \text{SiO}_2$ 1300 Glass	
F 199	49.84	36.39	5.23	8.24	60	25	15	1295 Glass + $2\text{CaO} \cdot \text{SiO}_2$ + $5\text{CaO} \cdot 3\text{Al}_2\text{O}_3$	
F 205	50.06	38.13	5.23	6.59	65	20	15	Crystallization too rapid for effective quenching	
F 206	49.75	39.14	4.53	6.59	67	20	13		
F 194	50.78	37.04	6.63	4.94	66	15	19	1340 Glass 1330 Glass + $2\text{CaO} \cdot \text{SiO}_2$ 1320 Glass + $2\text{CaO} \cdot \text{SiO}_2$ + $5\text{CaO} \cdot 3\text{Al}_2\text{O}_3$	

THE QUATERNARY SYSTEM

With the binary and ternary systems shown above, an exploration of the interior of the tetrahedron was now necessary. For this purpose, as explained previously, a series of pseudo-ternary systems was obtained, each system containing constant amounts respectively of 2, 5, 10 and 20% Fe_2O_3 . Except in the 20% Fe_2O_3 case, temperatures were too high to permit of complete exploration of the high lime region of the $\text{CaO}-\text{C}_2\text{S}-\text{C}_4\text{AF}$ side of the tetrahedron. In terms of $\text{CaO}-\text{C}_2\text{S}-\text{C}_4\text{AF}-\text{C}_5\text{A}_3$, the pseudo-ternary planes each contain constant amounts of C_4AF , the equivalent values being 6.1, 15.2, 30.4 and 60.8% respectively. It is in this form that the diagrams figs. 13-16 are plotted. Fig. 15a is a diagram of the system in terms of $\text{CaO}-\text{Al}_2\text{O}_3-\text{SiO}_2-\text{Fe}_2\text{O}_3$ and contains data on parts of the system, including the C_5A_3 field, which lies outside the smaller quaternary system.

Checks were also made on the base plane of $\text{CaO}-\text{Al}_2\text{O}_3-\text{SiO}_2$, *i.e.*, that investigated by RANKIN and WRIGHT, the checking points being mainly in the C_3S field and in the region round the $\text{CaO}-\text{C}_2\text{S}$ and $\text{C}_2\text{S}-\text{C}_3\text{S}$ boundary lines. The results for temperature and position of the boundary lines are in close agreement with the values taken from the RANKIN and WRIGHT diagram.

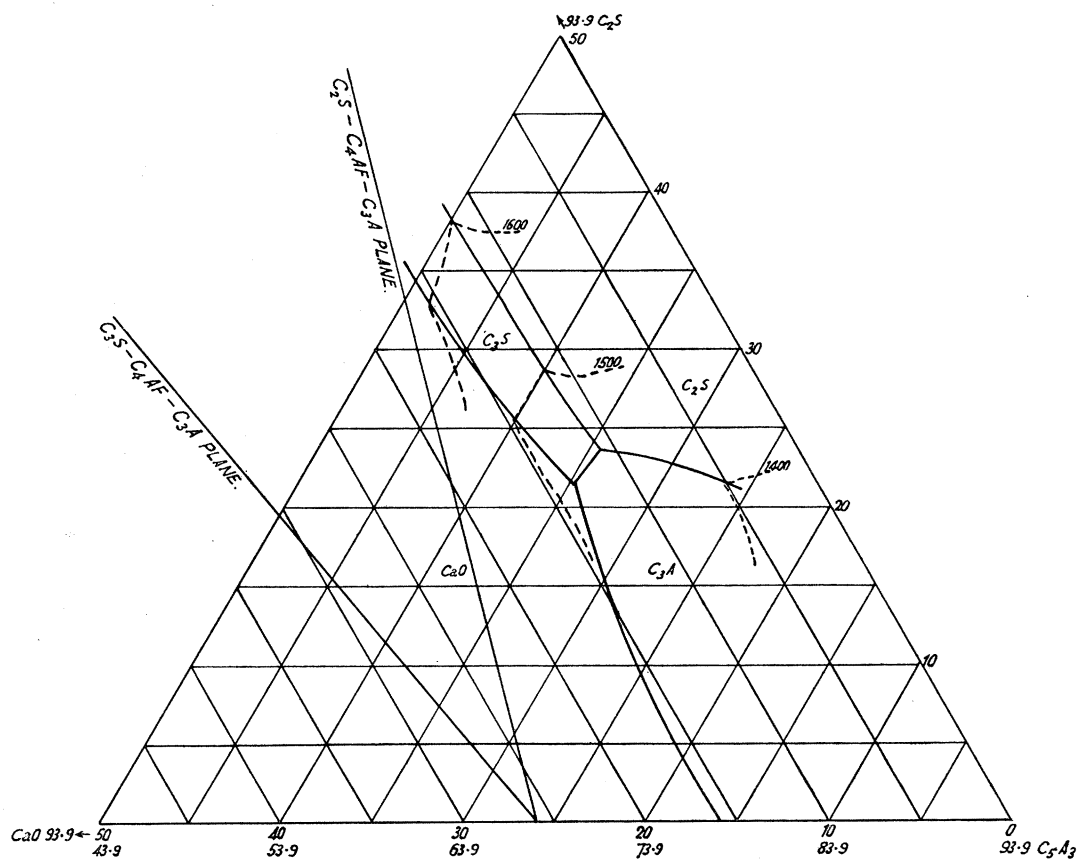


FIG. 13—System $\text{CaO}-\text{C}_2\text{S}-\text{C}_5\text{A}_3-\text{C}_4\text{AF}$. Plane through tetrahedron containing 6.1% C_4AF . Showing isotherms and intersections of the planes $\text{C}_2\text{S}-\text{C}_4\text{AF}-\text{C}_3\text{A}$ and $\text{C}_3\text{S}-\text{C}_4\text{AF}-\text{C}_3\text{A}$.

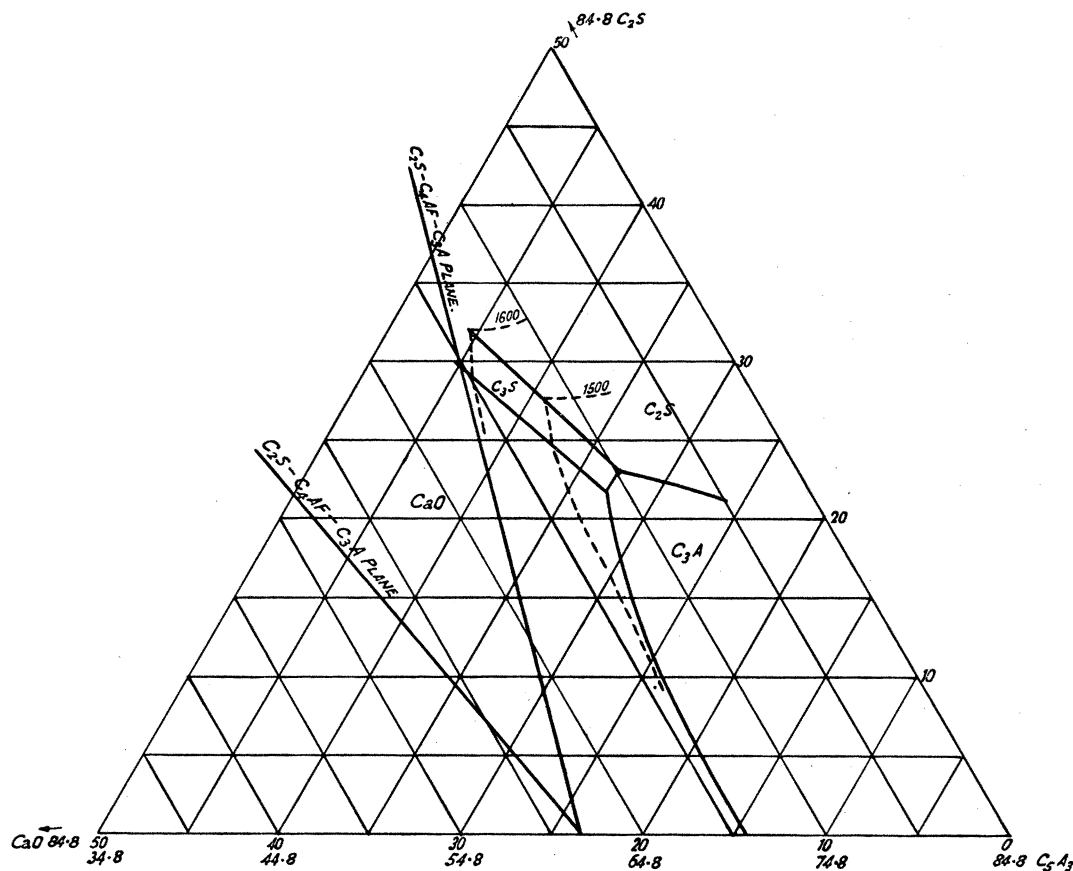


FIG. 14—Plane through tetrahedron containing 15.2% C_4AF . Showing isotherms and intersections of planes $C_2S-C_4AF-C_3A$ and $C_3S-C_4AF-C_3A$.

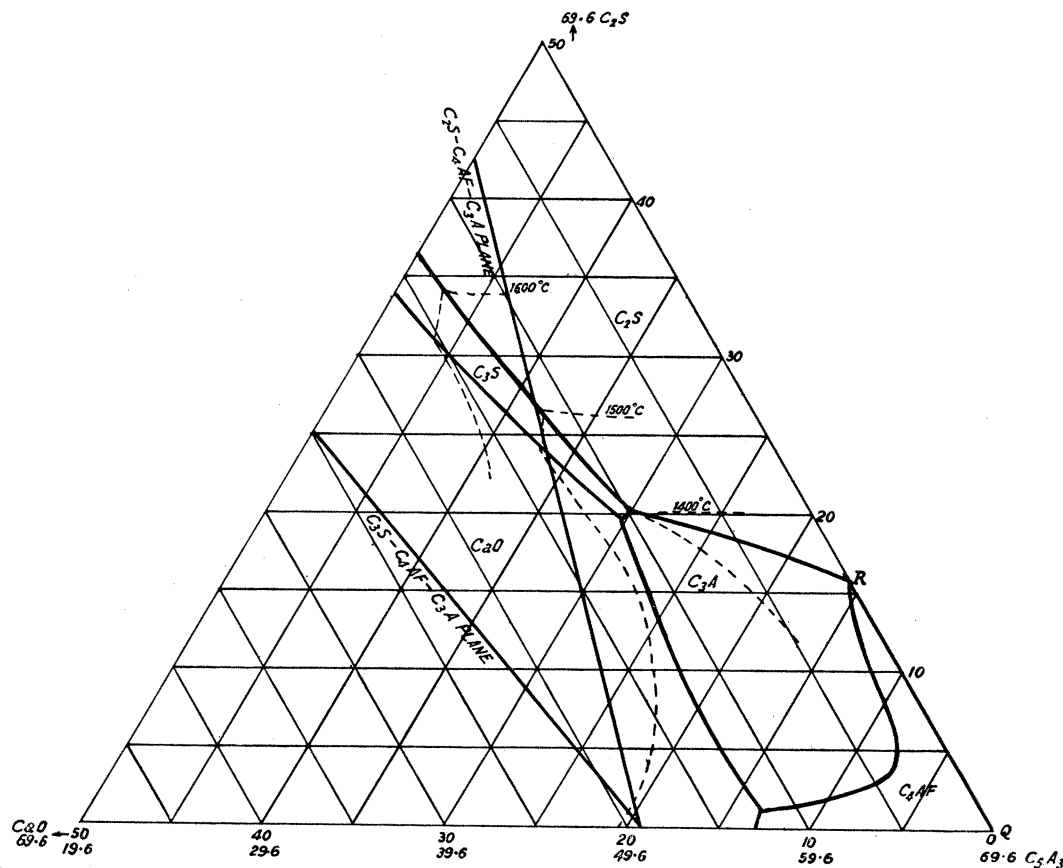


FIG. 15—Quaternary system $\text{CaO}-\text{C}_2\text{S}-\text{C}_5\text{A}_3-\text{C}_4\text{AF}$. Plane through tetrahedron in which percentage C_4AF in all mixes = 30.4. Showing isotherms and intersections of planes $C_2S-C_4AF-C_3A$ and $C_3S-C_4AF-C_3A$.

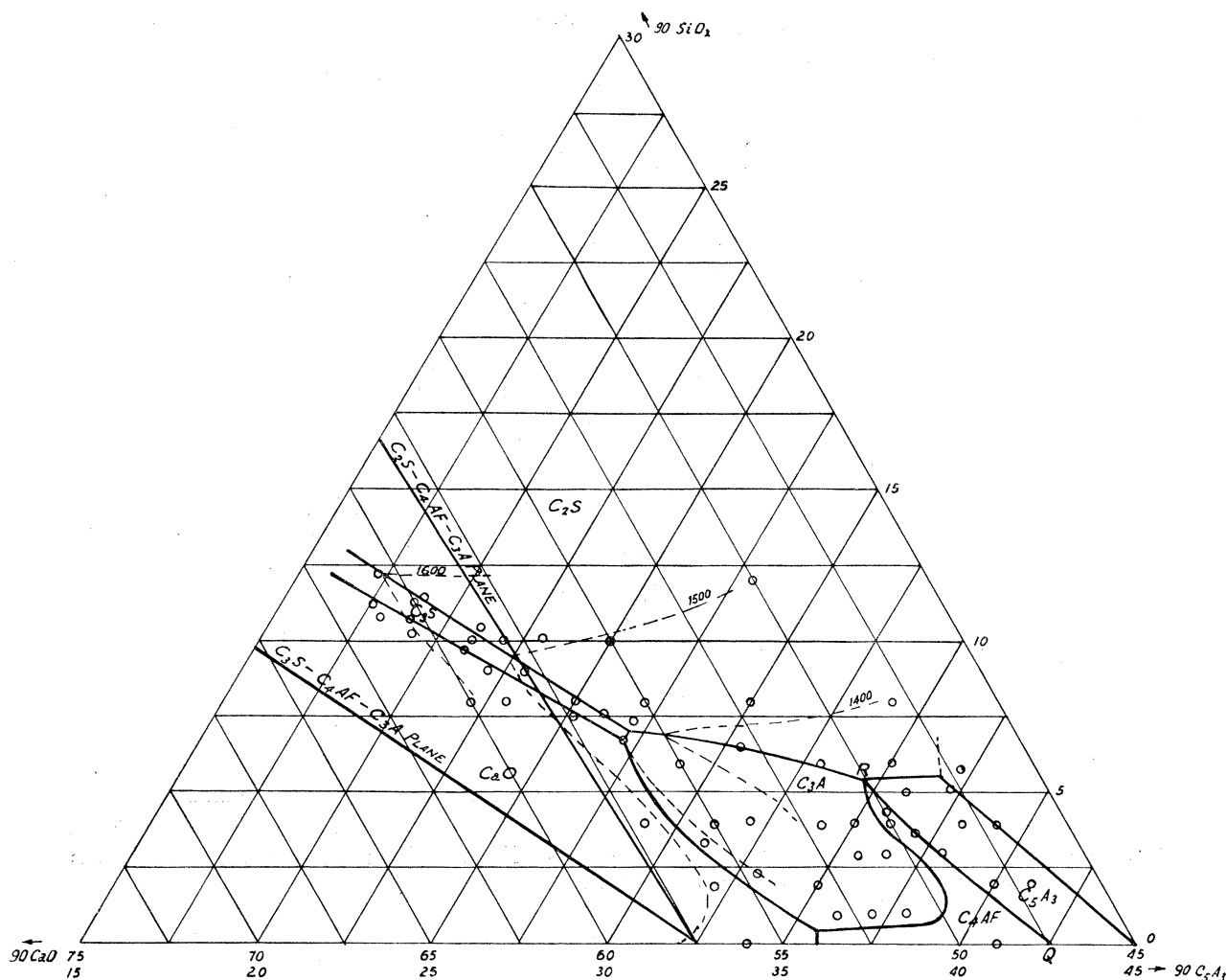


FIG. 15a—Portion of quaternary system $\text{CaO}-\text{Al}_2\text{O}_3-\text{SiO}_2-\text{Fe}_2\text{O}_3$. Plane in the tetrahedron containing 10% Fe_2O_3 . Showing compositions examined, isotherms, intersections of planes $\text{C}_2\text{S}-\text{C}_4\text{AF}-\text{C}_3\text{A}$ and $\text{C}_3\text{S}-\text{C}_4\text{AF}-\text{C}_3\text{A}$.

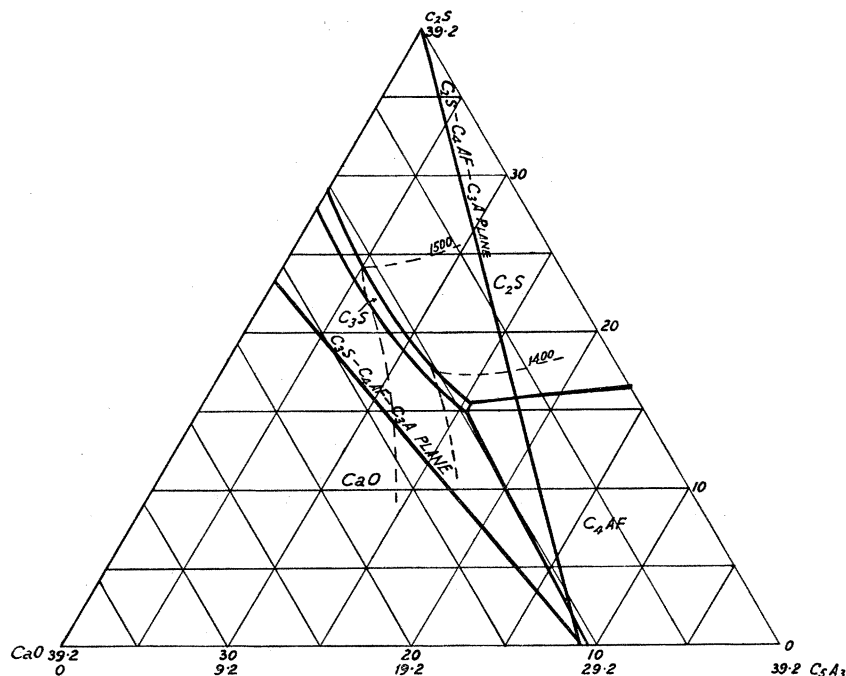


FIG. 16—Quaternary system $\text{CaO}-\text{C}_2\text{S}-\text{C}_5\text{A}_3-\text{C}_4\text{AF}$. Plane through tetrahedron in which percentage C_4AF in all compositions = 60.8. Showing isotherms and intersections of planes $\text{C}_2\text{S}-\text{C}_4\text{AF}-\text{C}_3\text{A}$ and $\text{C}_3\text{S}-\text{C}_4\text{AF}-\text{C}_3\text{A}$.

Data from which the diagrams were obtained is shown in Table V.

The system containing 10% Fe₂O₃ shows the C₃S field adjacent to the C₃A field, whereas the 20% Fe₂O₃ plane shows it now to be adjacent to the C₄AF field. The sextuple invariant points of the equilibrium of CaO, C₃S, C₃A and C₄AF and of C₃S, C₂S, C₃A and C₄AF must therefore lie between these two planes. To determine the ferric oxide content at which these points were to be found, a series of four compositions were made up on a line joining the composition point of C₄AF with the mid-point between the two quintuple points CaO—C₃S—C₃A and C₂S—C₃S—C₃A in the ternary system on the base plane. This line does not pass through the C₃S boundary surfaces against C₂A and C₄AF but lies close to it, making a small angle between the two. It was considered sufficiently near for the purpose required. Compositions containing 14, 15, 16 and 17% Fe₂O₃ were used and in observations by quenching, it was evident that the 17% point lay in the C₄AF volume, while the 14, 15 and 16% points were in the C₃A volume. Two additional compositions were prepared containing 14 and 16% Fe₂O₃, both compositions lying in the primary volume of CaO and close to the surface between CaO and either C₃A or C₄AF. Quench observations showed that the primary phase was in each case CaO while the second phase to crystallize was C₃A. It is concluded therefore that the Fe₂O₃ contents at the sextuple points are 16.5 ± 0.5% and by calculation, using data from figs. 13-16, compositions are:—CaO—C₃S—C₃A—C₄AF point (point T₁, figs. 20 and 21, Plate 1), CaO = 55.0%, Al₂O₃ = 22.7%, SiO₂ = 5.8%, Fe₂O₃ = 16.5%; C₃S—C₂S—C₃A—C₄AF point (point T₂), CaO = 54.8%, Al₂O₃ = 22.7%, SiO₂ = 6.0%, Fe₂O₃ = 16.5%. It is assumed that the two points have

TABLE V—Compositions defining the interior of the tetrahedron

(i) Compositions all containing 2% Fe₂O₃

Serial No.	Composition (remaining %)			Temperature	Quench data	
	CaO	Al ₂ O ₃	SiO ₂		Observed	
F 1	58.3	31.4	8.3	1470	Glass	
				1460	Glass + 3CaO . SiO ₂	
F 2	59.8	28.5	9.8	1520	Glass	
				1510	Glass + 3CaO . SiO ₂	
F 3	56.8	34.3	6.9	1450	Glass	
				1440	Glass + 3CaO . Al ₂ O ₃	
F 4	55.8	34.2	8.0	1430	Glass	
				1420	Glass + rare 2CaO . SiO ₂	
F 5	56.8	29.4	11.8	1530	Glass	
				1520	Glass + 2CaO . SiO ₂	
F 6	60.8	30.4	6.9	1590	Glass	
				1580	Glass + CaO	
F 7	61.7	24.0	12.3	1620	Glass	
				1610	Glass + 3CaO . SiO ₂	
F 8	58.8	28.4	10.8	1540	Glass + very rare 2CaO . SiO ₂	
F 9	60.8	24.5	12.7	1580	Glass	
				1570	Glass + 3CaO . SiO ₂	

TABLE V—(continued)

(i) Compositions all containing 2% Fe₂O₃—(continued)

Serial No.	Composition (remaining %)			Temperature	Quench data
	CaO	Al ₂ O ₃	SiO ₂		Observed
F 10	60.8	28.4	8.8	{ 1620 1600	Glass Glass + CaO
F 11	62.2	24.5	11.3	{ 1620 1600 1580	Glass Glass + CaO Glass + CaO + 3CaO . SiO ₂
F 12	59.8	25.3	12.9	{ 1590 1580	Glass Glass + occasional 2CaO . SiO ₂
F 13	59.8	26.5	11.8	{ 1540 1530	Glass Glass + 3CaO . SiO ₂
F 14	60.6	28.4	9.0	{ 1570 1560	Glass Glass + CaO
F 15	57.1	32.3	8.5	{ 1440 1430	Glass Glass + 2CaO . SiO ₂
F 16	53.9	37.2	6.9	{ 1390 1380	Glass Glass + rare 3CaO . Al ₂ O ₃
F 17	58.5	32.1	7.4	{ 1460 1450	Glass Glass + CaO
F 18	59.8	33.4	4.9	{ 1580 1480	Glass + CaO Glass + CaO + 3CaO . Al ₂ O ₃ (first appearance)
F 19	58.8	33.3	5.9	{ 1535 1525	Glass Glass + CaO
F 20	57.4	32.3	8.3	{ 1445 1435	Glass Glass + 2CaO . SiO ₂ + 3CaO . Al ₂ O ₃
F 21	58.1	32.4	7.5	{ 1455 1445	Glass Glass + 3CaO . Al ₂ O ₃
F 22	57.6	33.9	6.5	{ 1480 1460	Glass Glass + 3CaO . Al ₂ O ₃
F 23	57.8	35.8	4.4	{ 1530 1510	Glass Glass + CaO
F 24	58.6	35.5	4.0	{ 1530 1510	Glass + CaO Glass + CaO + 3CaO . Al ₂ O ₃

(ii) Compositions all containing 5% Fe₂O₃

F 25	56.5	30.4	8.1	{ 1440 1430	Glass + 2CaO . SiO ₂ Glass + 2CaO . SiO ₂ + 3CaO . Al ₂ O ₃
F 26	57.9	27.6	9.5	{ 1500 1480	Glass Glass + 2CaO . SiO ₂

QUATERNARY SYSTEM $\text{CaO}-\text{Al}_2\text{O}_3-\text{SiO}_2-\text{Fe}_2\text{O}_3$

25

TABLE V—(continued)

(ii) Compositions all containing 5% Fe_2O_3 —(continued)

Serial No.	Composition (remaining %)			Temperature	Quench data
	CaO	Al_2O_3	SiO_2		Observed
F 27	59.6	23.7	11.7	1600	Glass + very rare $2\text{CaO} \cdot \text{SiO}_2$
F 28	57.9	24.7	12.4	{ 1600 1590	Glass Glass + $2\text{CaO} \cdot \text{SiO}_2$
F 29	56.1	28.5	10.5	{ 1550 1540	Glass Glass + $2\text{CaO} \cdot \text{SiO}_2$
F 31	57.9	30.4	6.7	{ 1540 1530	Glass Glass + CaO
F 32	58.7	27.7	8.6	{ 1580 1560	Glass Glass + rare CaO
F 33	60.3	23.8	10.9	{ 1620 1610	Glass Glass + CaO
F 34	54.1	33.3	7.6	{ 1440 1430	Glass Glass + $2\text{CaO} \cdot \text{SiO}_2$
F 35	58.2	27.8	9.0	{ 1510 1500	Glass Glass + $3\text{CaO} \cdot \text{SiO}_2$
F 36	59.6	26.0	9.4	{ 1565 1555	Glass Glass + rare CaO
F 37	57.0	30.4	7.6	{ 1440 1430	Glass Glass + $2\text{CaO} \cdot \text{SiO}_2$
F 38	57.0	31.0	7.0	{ 1460 1440	Glass Glass + $2\text{CaO} \cdot \text{SiO}_2$
F 39	59.6	23.8	11.7	1600	Glass + $2\text{CaO} \cdot \text{SiO}_2$
F 40	60.4	25.0	9.6	{ 1590 1570	Glass Glass + CaO
F 43	55.6	32.0	7.4	{ 1445 1435	Glass Glass + $3\text{CaO} \cdot \text{Al}_2\text{O}_3$
F 44	55.0	32.0	8.0	{ 1440 1430	Glass Glass + rare $3\text{CaO} \cdot \text{Al}_2\text{O}_3$
F 46	58.4	26.0	10.6	1500	Glass + $2\text{CaO} \cdot \text{SiO}_2$
F 45 ii	59.0	26.0	10.0	{ 1580 1570	Glass Glass + very rare $2\text{CaO} \cdot \text{SiO}_2$
F 47	57.6	29.6	7.8	{ 1480 1470 1500	Glass Glass + $3\text{CaO} \cdot \text{SiO}_2$ Glass
F 48	54.5	32.0	8.5	{ 1490	Glass + very rare $2\text{CaO} \cdot \text{SiO}_2$
F 49	53.0	35.0	7.0	{ 1440 1430	Glass Glass + $2\text{CaO} \cdot \text{SiO}_2$
F 50	53.7	35.0	6.3	{ 1430 1420	Glass Glass + $3\text{CaO} \cdot \text{Al}_2\text{O}_3$
F 51	55.4	31.6	8.0	1470	Glass + rare $2\text{CaO} \cdot \text{SiO}_2$

TABLE V—(continued)

(iii) Compositions all containing 10% Fe_2O_3

Serial No.	Composition (remaining %)			Temperature	Quench data
	CaO	Al_2O_3	SiO_2		Observed
F 56	57.0	29.0	4.0	1550	Glass
				1540	Glass + CaO
				1460	Glass + CaO + $3\text{CaO} \cdot \text{Al}_2\text{O}_3$
F 57	54.0	32.0	4.0	1430	Glass
				1420	Glass + $3\text{CaO} \cdot \text{Al}_2\text{O}_3$
				1340	Glass
F 58	50.0	36.0	4.0	1330	Glass + $4\text{CaO} \cdot \text{Al}_2\text{O}_3 \cdot \text{Fe}_2\text{O}_3$
				1320	Glass + $4\text{CaO} \cdot \text{Al}_2\text{O}_3 \cdot \text{Fe}_2\text{O}_3 + 5\text{CaO} \cdot 3\text{Al}_2\text{O}_3$
F 59	47.0	39.0	4.0	1340	Glass
F 60	55.0	27.0	8.0	1330	Glass + $5\text{CaO} \cdot 3\text{Al}_2\text{O}_3$
F 61	52.0	30.0	8.0	1450	Glass
				1440	Glass + $2\text{CaO} \cdot \text{SiO}_2$
F 62	48.0	34.0	8.0	1470	Glass
				1460	Glass + $2\text{CaO} \cdot \text{SiO}_2$
F 63	50.0	28.0	12.0	1390	Glass
				1380	Glass + $2\text{CaO} \cdot \text{SiO}_2$
F 64	47.0	41.0	2.0	1500	Glass
				1490	Glass + $2\text{CaO} \cdot \text{SiO}_2$
F 65	48.0	40.0	2.0	1330	Glass
				1320	Glass + $5\text{CaO} \cdot 3\text{Al}_2\text{O}_3$
F 66	53.0	35.0	2.0	1340	Glass
				1330	Glass + $5\text{CaO} \cdot 3\text{Al}_2\text{O}_3 + 4\text{CaO} \cdot \text{Al}_2\text{O}_3 \cdot \text{Fe}_2\text{O}_3$
F 67	56.0	32.0	2.0	1420	Glass
F 68	48.0	38.0	4.0	1410	Glass + $3\text{CaO} \cdot \text{Al}_2\text{O}_3$
				1510	Glass + very rare CaO
F 69	52.0	34.0	4.0	1330	Glass
				1320	Glass + very rare $5\text{CaO} \cdot 3\text{Al}_2\text{O}_3$
F 70	50.0	35.0	5.0	1380	Glass
				1370	Glass + $3\text{CaO} \cdot \text{Al}_2\text{O}_3$
F 71	49.0	35.0	6.0	1310	Glass
				1300	Glass + $4\text{CaO} \cdot \text{Al}_2\text{O}_3 \cdot \text{Fe}_2\text{O}_3$
F 72	51.0	33.0	6.0	1325	Glass
				1310	Glass + $2\text{CaO} \cdot \text{SiO}_2$
F 74	47.2	37.0	5.8	1350	Glass
				1340	Glass + $2\text{CaO} \cdot \text{SiO}_2$
				1310	Glass
				1300	Glass + $\text{CaO} \cdot \text{Al}_2\text{O}_3$

QUATERNARY SYSTEM $\text{CaO}-\text{Al}_2\text{O}_3-\text{SiO}_2-\text{Fe}_2\text{O}_3$

27

TABLE V—(continued)

(iii) Compositions all containing 10% Fe_2O_3 —(continued)

Serial No.	Composition (remaining %)			Temperature	Quench data
	CaO	Al_2O_3	SiO_2		Observed
F 75	47.8	37.0	5.2	{ 1310 1300	Glass Glass + $5\text{CaO} \cdot 3\text{Al}_2\text{O}_3$
F 76	49.2	35.6	5.2	{ 1310 1300	Glass Glass + $5\text{CaO} \cdot 3\text{Al}_2\text{O}_3$
F 77	51.0	35.0	4.0	{ 1340 1330	Glass Glass + $3\text{CaO} \cdot \text{Al}_2\text{O}_3$
F 78	53.0	30.6	6.4	{ 1360 1350 1340	Glass Glass + $2\text{CaO} \cdot \text{SiO}_2$ Glass + $2\text{CaO} \cdot \text{SiO}_2$ + $3\text{CaO} \cdot \text{Al}_2\text{O}_3$
F 79	55.0	31.0	4.0	{ 1430 1420	Glass Glass + $3\text{CaO} \cdot \text{Al}_2\text{O}_3$
F 80	55.6	27.0	7.4	{ 1430 1420	Glass Glass + $2\text{CaO} \cdot \text{SiO}_2$
F 81	56.2	27.0	6.8	{ 1400 1390	Glass Glass + $3\text{CaO} \cdot \text{SiO}_2$ + $2\text{CaO} \cdot \text{SiO}_2$
F 82	59.0	23.0	8.0	{ 1570 1550	Glass Glass + CaO
F 83	58.0	23.0	9.0	{ 1510 1500	Glass Glass + $3\text{CaO} \cdot \text{SiO}_2$
F 84	56.7	23.1	10.1	{ 1530 1520	Glass Glass + $2\text{CaO} \cdot \text{SiO}_2$
F 85	60.0	22.0	8.0	1540	Glass + CaO
F 86	59.0	22.0	9.0	{ 1530 1520	Glass Glass + CaO
F 87	58.0	22.0	10.0	{ 1530 1520	Glass Glass + $2\text{CaO} \cdot \text{SiO}_2$
F 88	57.0	25.0	8.0	{ 1470 1460	Glass Glass + $3\text{CaO} \cdot \text{SiO}_2$
F 89	57.3	25.2	7.5	{ 1430 1410	Glass Glass + CaO
F 90	56.8	25.9	7.2	{ 1490 1480	Glass Glass + rare $2\text{CaO} \cdot \text{SiO}_2$
F 91	56.4	26.0	7.6	{ 1430 1420	Glass Glass + $2\text{CaO} \cdot \text{SiO}_2$
F 93	59.0	21.0	10.0	{ 1520 1510	Glass Glass + $3\text{CaO} \cdot \text{SiO}_2$ + $2\text{CaO} \cdot \text{SiO}_2$
F 94	59.4	21.0	9.6	{ 1530 1520	Glass Glass + $3\text{CaO} \cdot \text{SiO}_2$
F 95	58.6	21.0	10.4	{ 1530 1520	Glass Glass + $2\text{CaO} \cdot \text{SiO}_2$
F 98	54.6	33.0	2.4	{ 1400 1390	Glass Glass + $3\text{CaO} \cdot \text{Al}_2\text{O}_3$

TABLE V—(continued)

(iii) Compositions all containing 10% Fe_2O_3 —(continued)

Serial No.	Composition (remaining %)			Temperature	Quench data
	CaO	Al_2O_3	SiO_2		Observed
F 99	55.6	31.0	3.4	{ 1360 1350	Glass Glass + $3\text{CaO} \cdot \text{Al}_2\text{O}_3$
F 100	51.4	35.6	3.0	{ 1350 1340	Glass Glass + $3\text{CaO} \cdot \text{Al}_2\text{O}_3$
F 101	49.0	38.0	3.0	{ 1320 1310	Glass Glass + $5\text{CaO} \cdot 3\text{Al}_2\text{O}_3$
F 102	59.6	19.0	11.4	1580	Glass + rare $2\text{CaO} \cdot \text{SiO}_2$
F 103	60.0	18.8	11.2	{ 1560 1550	Glass Glass + $3\text{CaO} \cdot \text{SiO}_2$
F 104	60.4	19.0	10.6	{ 1600 1580	Glass Glass + $3\text{CaO} \cdot \text{SiO}_2$
F 105	60.6	19.2	10.2	{ 1600 1580	Glass Glass + CaO
F 106	60.2	17.8	12.0	{ 1590 1580	Glass Glass + $2\text{CaO} \cdot \text{SiO}_2$ + rare $3\text{CaO} \cdot \text{SiO}_2$
F 107	60.6	17.4	12.0	1600	Glass + $2\text{CaO} \cdot \text{SiO}_2$ + doubtful $3\text{CaO} \cdot \text{SiO}_2$
F 108	61.2	17.6	11.2	1600	Glass + CaO
F 109	61.2	18.0	10.8	1600	Glass + CaO
F 110	50.6	36.4	3.0	{ 1340 1330	Glass Glass + $3\text{CaO} \cdot \text{Al}_2\text{O}_3$
F 112	53.0	36.0	1.0	{ 1430 1420	Glass Glass + very rare $3\text{CaO} \cdot \text{Al}_2\text{O}_3$
F 113	52.0	37.0	1.0	{ 1390 1380	Glass Glass + $3\text{CaO} \cdot \text{Al}_2\text{O}_3$
F 114	51.0	38.0	1.0	{ 1350 1340	Glass Glass + $3\text{CaO} \cdot \text{Al}_2\text{O}_3$

(iv) Compositions all containing 20% Fe_2O_3

F 130	51.0	23.0	6.0	{ 1360 1350	Glass Glass + $2\text{CaO} \cdot \text{SiO}_2$
F 131	51.0	22.0	7.0	{ 1460 1450	Glass Glass + $2\text{CaO} \cdot \text{SiO}_2$
F 132	52.0	22.0	6.0	{ 1370 1360 1350	Glass Glass + $2\text{CaO} \cdot \text{SiO}_2$ Glass + $2\text{CaO} \cdot \text{SiO}_2$ + $4\text{CaO} \cdot \text{Al}_2\text{O}_3 \cdot \text{Fe}_2\text{O}_3$
F 133	51.0	21.0	8.0	{ 1440 1430	Glass Glass + $2\text{CaO} \cdot \text{SiO}_2$
F 134	52.0	21.0	7.0	{ 1400 1390	Glass Glass + $2\text{CaO} \cdot \text{SiO}_2$

QUATERNARY SYSTEM $\text{CaO}-\text{Al}_2\text{O}_3-\text{SiO}_2-\text{Fe}_2\text{O}_3$

29

TABLE V—(continued)

(iv) Compositions all containing 20% Fe_2O_3 —(continued)

Serial No.	Composition (remaining %)			Temperature	Quench data
	CaO	Al_2O_3	SiO_2		Observed
F 135	53.0	21.0	6.0	{ 1370 1360	Glass Glass + rare $2\text{CaO} \cdot \text{SiO}_2$
F 136	52.0	20.0	8.0	{ 1480 1470	Glass Glass + $2\text{CaO} \cdot \text{SiO}_2$
F 137	53.0	20.0	7.0	{ 1450 1440	Glass Glass + $2\text{CaO} \cdot \text{SiO}_2$
F 138	53.0	19.0	8.0	{ 1460 1450	Glass Glass + $2\text{CaO} \cdot \text{SiO}_2$
F 139	53.4	20.0	6.6	{ 1450 1440	Glass Glass + $2\text{CaO} \cdot \text{SiO}_2$
F 140	54.0	19.0	7.0	{ 1450 1440	Glass Glass + $2\text{CaO} \cdot \text{SiO}_2$
F 141R	55.0	19.0	6.0	{ 1390 1380	Glass Glass + very rare $2\text{CaO} \cdot \text{SiO}_2$
F 142	54.0	18.0	8.0	1450	Glass + $2\text{CaO} \cdot \text{SiO}_2$
F 143	55.0	18.0	7.0	1410	Glass + $2\text{CaO} \cdot \text{SiO}_2$
F 144	55.0	17.0	8.0	1450	Glass + $2\text{CaO} \cdot \text{SiO}_2$
F 146	56.0	16.0	8.0	{ 1490 1480 1470	Glass Glass + rare $2\text{CaO} \cdot \text{SiO}_2$ Glass + $2\text{CaO} \cdot \text{SiO}_2$ + $3\text{CaO} \cdot \text{SiO}_2$
F 147	57.0	16.0	7.0	{ 1450 1430	Glass + CaO Glass + CaO + $3\text{CaO} \cdot \text{SiO}_2$
F 148	58.0	16.0	6.0	1450	Glass + CaO
F 149	59.0	16.0	5.0	1520	Glass + CaO
F 150	57.0	19.0	4.0	1520	Glass + CaO
F 151	56.0	18.0	6.0	{ 1450 1370	Glass + CaO Glass + CaO + $3\text{CaO} \cdot \text{SiO}_2$
F 152	56.0	19.0	5.0	{ 1450 1360	Glass + CaO Glass + CaO + $3\text{CaO} \cdot \text{SiO}_2$
F 153	54.0	21.0	5.0	{ 1350 1340	Glass Glass + occasional $4\text{CaO} \cdot \text{Al}_2\text{O}_3 \cdot \text{Fe}_2\text{O}_3$
F 154	55.0	21.0	4.0	{ 1360 1350 1345	Glass + CaO Glass + CaO + $4\text{CaO} \cdot \text{Al}_2\text{O}_3 \cdot \text{Fe}_2\text{O}_3$ Glass + CaO + $4\text{CaO} \cdot \text{Al}_2\text{O}_3 \cdot \text{Fe}_2\text{O}_3$ + $3\text{CaO} \cdot \text{SiO}_2$
F 157	55.5	18.0	6.5	{ 1340 1410 1400	All crystalline Glass Glass + $2\text{CaO} \cdot \text{SiO}_2$

TABLE V—(continued)

(iv) Compositions all containing 20% Fe_2O_3 —(continued)

Serial No.	Composition (remaining %)			Temperature	Quench data
	CaO	Al_2O_3	SiO_2		Observed
F 158	56.0	17.0	7.0	{ 1440 1430	Glass Glass + 3CaO . SiO_2
F 159	56.5	16.0	7.5	1500	Glass + CaO
F 160	56.8	15.1	8.0	1540	Glass + CaO
F 161	55.0	19.4	5.6	{ 1400 1390	Glass Glass + rare CaO
F 163	54.4	20.0	5.6	{ 1360 1350	Glass Glass + 3CaO . SiO_2
F 164	54.0	22.0	4.0	1380	Glass + CaO
F 165	53.4	22.7	3.9	{ 1360 1350	Glass Glass + 4CaO . Al_2O_3 . Fe_2O_3
F 166	53.0	24.0	3.0	{ 1370 1360	Glass Glass + 4CaO . Al_2O_3 . Fe_2O_3
F 167	51.0	25.0	4.0	{ 1360 1350	Glass Glass + 4CaO . Al_2O_3 . Fe_2O_3

(v) Compositions all containing 23% Fe_2O_3

F 171	54.0	19.0	4.0	{ 1400 1360	Glass Glass + 4CaO . Al_2O_3 . Fe_2O_3
F 172	53.0	19.0	5.0	{ 1400 1360	Glass + CaO Glass + CaO + 4CaO . Al_2O_3 . Fe_2O_3
F 173	52.0	19.0	6.0	{ 1400 1320	Glass + rare 2CaO . SiO_2 Glass + 2CaO . SiO_2 + 4CaO . Al_2O_3 . Fe_2O_3
F 174	51.0	19.0	7.0	{ 1400 1360	Glass + 2CaO . SiO_2 Glass + 2CaO . SiO_2 + considerable 4CaO . Al_2O_3 . Fe_2O_3
F 177	56.0	16.0	5.0	{ 1440 1400 1360	Glass + CaO Glass + CaO + 3CaO . SiO_2 Glass + CaO + 3CaO . SiO_2 + 4CaO . Al_2O_3 . Fe_2O_3
F 178	55.0	16.0	6.0	{ 1440 1400	Glass Glass + 3CaO . SiO_2
F 179	54.0	16.0	7.0	{ 1440 1400	Glass Glass + 2CaO . SiO_2 + 3CaO . SiO_2
F 180	53.0	16.0	8.0	1440	Glass + 2CaO . SiO_2

QUATERNARY SYSTEM $\text{CaO—Al}_2\text{O}_3\text{—SiO}_2\text{—Fe}_2\text{O}_3$

31

TABLE V—(continued)

(vi) Compositions to determine position of sextuple point

Serial No.	Composition				Temperature	Quench data
	CaO	Al_2O_3	SiO_2	Fe_2O_3		Observed
F 155	53.5	27.9	4.6	14.0	1360	Glass + considerable $3\text{CaO} \cdot \text{Al}_2\text{O}_3$
F 169	53.1	27.5	4.4	15.0	{ 1350 1340	Glass Glass + very rare $3\text{CaO} \cdot \text{Al}_2\text{O}_3$
F 170	52.7	27.2	4.1	16.0	{ 1350 1340	Glass Glass + very rare $3\text{CaO} \cdot \text{Al}_2\text{O}_3$
F 156	52.4	26.8	3.9	17.0	{ 1340 1320	Glass Glass + $4\text{CaO} \cdot \text{Al}_2\text{O}_3 \cdot \text{Fe}_2\text{O}_3$
F 209	56.2	25.2	4.6	14.0	{ 1400 1370	Glass + CaO Glass + CaO + $3\text{CaO} \cdot \text{Al}_2\text{O}_3$
F 210	55.8	23.8	4.4	16.0	{ 1370 1360	Glass + CaO Glass + CaO + $3\text{CaO} \cdot \text{Al}_2\text{O}_3$

(vii) Compositions on the base plane $\text{CaO—Al}_2\text{O}_3\text{—SiO}_2$

Serial No.	Composition			Temperature	Quench data
	CaO	Al_2O_3	SiO_2		Observed
12'	62.0	31.0	7.0	{ 1600 1580	Glass Glass + CaO
13'	63.5	25.0	11.5	1600	Glass + CaO + $3\text{CaO} \cdot \text{SiO}_2$
14'	63.0	25.0	12.0	1580	Glass + $3\text{CaO} \cdot \text{SiO}_2$
16'	62.0	28.0	10.0	{ 1580 1560	Glass Glass + $3\text{CaO} \cdot \text{SiO}_2$
6'	59.5	32.0	8.5	{ 1500 1490	Glass Glass + $3\text{CaO} \cdot \text{SiO}_2$
7'	61.0	29.0	10.0	{ 1570 1560	Glass Glass + $3\text{CaO} \cdot \text{SiO}_2$
17'	61.0	28.0	11.0	{ 1580 1560	Glass Glass + $3\text{CaO} \cdot \text{SiO}_2$ + $2\text{CaO} \cdot \text{SiO}_2$
15'	62.0	25.0	13.0	1580	Glass + $2\text{CaO} \cdot \text{SiO}_2$
18'	60.5	28.0	11.5	{ 1580 1550	Glass Glass + $2\text{CaO} \cdot \text{SiO}_2$
10'	56.9	34.9	8.2	{ 1470 1460	Glass Glass + $2\text{CaO} \cdot \text{SiO}_2$
11'	58.0	30.0	12.0	{ 1580 1570	Glass Glass + $2\text{CaO} \cdot \text{SiO}_2$
8'	58.0	35.0	7.0	{ 1480 1470	Glass Glass + $3\text{CaO} \cdot \text{Al}_2\text{O}_3$

about the same iron contents and lie on a plane parallel to the base $\text{CaO}-\text{Al}_2\text{O}_3-\text{SiO}_2$ plane. Heating curves on suitable mixes showed point T_1 to have a temperature of $1341 \pm 5^\circ \text{C}$ and point T_2 to be at $1338 \pm 3^\circ \text{C}$.

In the 10% Fe_2O_3 plane (figs. 15 and 15*a*) a point R is shown in which C_5A_3 , C_3A , C_4AF and C_2S are in equilibrium, and this point therefore appears to be the sextuple point for these four compounds. The composition is $\text{CaO} = 50.0\%$, $\text{Al}_2\text{O}_3 = 34.5\%$, $\text{SiO}_2 = 5.5\%$, $\text{Fe}_2\text{O}_3 = 10.0\%$ with a temperature of melting as $1280 \pm 5^\circ \text{C}$ from heating curves and quenches.

With the data obtained above, construction of a complete three dimensional diagram can now be made. In figs. 20 and 21, Plate 1 is shown what is probably the simplest method of construction, in which the quintuple lines and invariant points only are shown and the direction of falling temperature along these indicated by arrows.

Surfaces showing temperature isotherms can also be inserted either by means of "Cellophane" or by indicating the surface with wire strands, but the added complexity makes it impossible to secure a clear photograph. No plate is therefore shown of this, but the necessary data are present in figs. 13-16.

The primary volume of CaO occupies the greater part of the tetrahedron. The volumes of C_2S and C_4AF do not present any unusual features, but in the case of the primary volume of C_5A_3 , the quaternary invariant point for the equilibrium of C_5A_3 , C_3A , C_2S , and C_4AF coincides with the ternary eutectic at which C_5A_3 , C_2S , and C_4AF are in equilibrium, within the accuracy available experimentally. It is interesting to note that HANSEN, BROWNMILLER, and BOGUE (see fig. 9) found that the binary eutectic of the system $C_4AF-C_5A_3$ was also identical, within experimental error, with the ternary eutectic of C_3A , C_5A_3 , and C_4AF . In effect, the $C_5A_3-C_3A-C_4AF$ quintuple line (QR) lies almost in the $C_4AF-C_5A_3-C_2S$ plane. Hence the ternary eutectic of $C_4AF-C_5A_3-C_3A$ is practically superimposed on the $C_4AF-C_5A_3$ binary eutectic (Q) and the $C_4AF-C_5A_3-C_3A-C_2S$ invariant point on the $C_4AF-C_5A_3-C_2S$ ternary eutectic (R). It is probable that actually these eutectics are not identical points, but the experimental accuracy is not sufficient to differentiate between them.* The C_3S volume is narrow and skew shaped and as it approaches the C_3S composition thins out to a wedge, the edge of which forms the $C_2S-C_3S-\text{CaO}$ quintuple line. This line is also an edge of the $C_2S-\text{CaO}$ boundary surface.

The primary volume of C_3S shows other interesting features. Pure C_3S is a compound unstable below its melting point, dissociating at 1900°C into C_2S and CaO . It does not appear as a primary phase in the binary system $\text{CaO}-\text{SiO}_2$, the liquid temperatures being above 1900°C , while in the ternary system of $\text{CaO}-\text{Al}_2\text{O}_3-\text{SiO}_2$, the primary field narrows with increasing temperature until finally, at 1900° , it disappears and a boundary line between CaO and C_2S takes its place.

* If these eutectics are identical in composition, then C_3A is an "indifferent" phase in the sense of SCHREINEMAKER.

CARLSON(*) has recently shown that C_3S is also unstable at some lower temperature. In his experiments amounts of C_3S were heated for a standard time at different temperatures, the resulting product being analysed for free CaO. A graph was obtained of free lime against temperature which showed amounts of free lime rising to a maximum at 1175°C and falling away with increasing temperature, becoming practically zero at 1300°C . This diagram must be regarded as a rate graph and does not involve equilibrium conditions; a graph at equilibrium would show a sharp break at the temperature of decomposition. As JÄNECKE† has pointed out, with a suitable fluxing third component, a ternary system with CaO and C_2S might be obtained in which the field of C_3S narrowed to a point at both ends, meeting the boundary line between CaO and C_2S in a quintuple point. The addition of a fourth component with a sufficient fluxing action on the system $\text{CaO—Al}_2\text{O}_3\text{—SiO}_2$ might be expected to have a similar effect on the C_3S volume, causing it to narrow to an edge at the lower temperature part, the edge being a quintuple line meeting a $\text{CaO—}C_2S$ boundary surface. This would appear first on the boundary surface between C_3S and C_3A or C_4AF ; these surfaces, $C_3S\text{—}C_3A$ and $C_3S\text{—}C_4AF$, would not then meet but would each taper to points which would be joined by a quintuple line along which CaO, C_2S , and C_3S existed in equilibrium. The quintuple line would not be in the same plane as the C_3S surfaces against C_3A and C_4AF , but would appear after the fashion shown in fig. 17*b*.

The actual shape of the surfaces $C_3S\text{—}C_3A$ and $C_3S\text{—}C_4AF$ which happen to fall in one plane is shown in fig. 17, which is a drawing to scale from the solid model. Fig. 17*a* also shows this in an exaggerated form, in which the horizontal scale has been increased. With increase of Fe_2O_3 it is clear that there is a pronounced narrowing of the surface between C_3S and C_3A , but successive results from the 10, 20, and 23% Fe_2O_3 planes shows that C_3S still appears as a primary phase, though at 10 and 20% Fe_2O_3 , the surface only covers a width represented by 0.2% SiO_2 . The surface narrows as the temperature decreases, and as the points T_1 and T_2 are at the lowest temperature on their respective quintuple lines, the surface may be expected to be narrowest at this point. In effect, however, there can be little difference in the width from T_1 T_2 to XW because the temperature gradient is very small.

Since the fusion relations in the quaternary system showed that C_3S remained stable in contact with liquid down to the sextuple point, some additional experiments were carried out at temperatures below that of liquid formation in this part of the system. Melts F 106 and F 107 were chosen, in which, by decomposition of C_3S , potential amounts of 5 and 6% of free CaO, respectively, could be developed. Tests on the melt as originally prepared showed no free lime to be present. Successive amounts of the materials were filled into small platinum crucibles and maintained at constant temperature for definite periods, during each of which

* 'U.S. Bur. Stands. J. Res.,' vol. 7, p. 893 (1931).

† 'Zement,' vol. 21, p. 377 (1932).

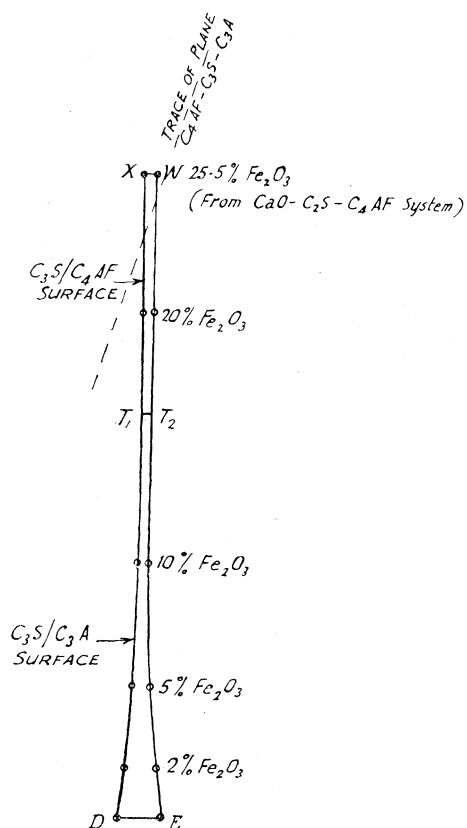


FIG. 17—Boundary surface of C_3S against C_3A and C_4AF . Drawn to scale from the model and from figs. 13-16.

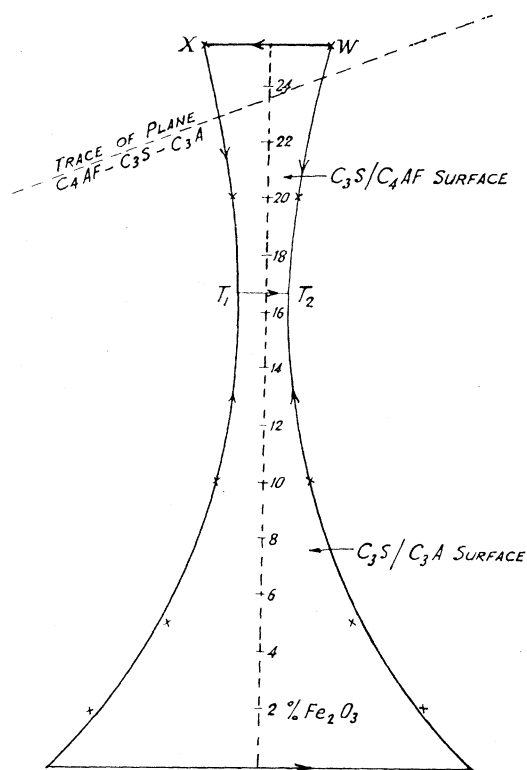


FIG. 17a—Boundary surface of C_3S against $C_3A - C_4AF$. Scale of width 10 times that of fig. 17. Arrows show direction of falling temperature.

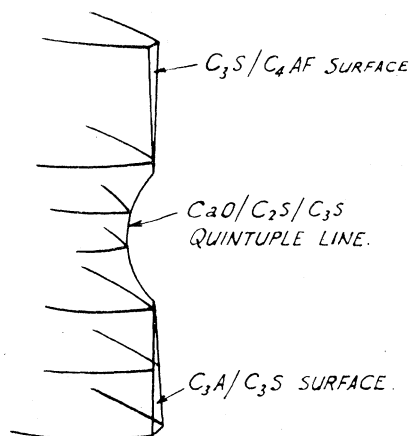


FIG. 17b—Hypothetical diagram of C_3S surface against C_3A and C_4AF if C_3S decomposes at temperatures when liquid is present.

periods, the percentage of free lime was estimated from time to time.* Similar tests were also carried out on pure C_3S . Table VI gives the results obtained.

TABLE VI

Material	Temperature of heating °C	Time of heating hours	Free lime developed %	C_3S decomposed %
F 106	1150	240	3.84	76.9
	1175(i)	48	0.54	10.8
		240	3.84	76.9
	1175(ii)	150	3.54	70.9
		300	4.62	92.5
	1225	220	1.2	24.0
	1250	48	0	0
1300	90	0	0	
F 107	1225	100	0.3	5.0
		200	3.1	51.6
		300	4.0	66.7
	1250	100	1.0	16.7
		200	0.0	0.0
		300	1.0	16.7
	1300	100	0	0
1350	100	0	0	
C_3S	1175	108	1.9	7.7
		300	4.4	17.9
		640	21.0	85.5
	1200	200	15.5	63.0
	1225	100	1.0	4.0
		150	4.0	17.1
1250	120	0	0	
1275	140	0	0	

The error in the determination of free CaO for F 106 and F 107 is of the order of $\pm 0.2\%$. It is evident that the sharp decomposition temperature required on Phase Rule considerations, for a compound, is verified. The rate of decomposition, however, is very slow and only in one case has practically complete decomposition of the compound been obtained.

It is concluded that the lower decomposition occurs at a temperature of $1250 \pm 25^\circ \text{C}$.

This example of a compound stable only between two definite temperature limits and decomposing to the same products above and below the stability limits appears to be unique.

A consideration of the free energy-temperature relations for CaO , $3\text{CaO} \cdot \text{SiO}_2$ and $2\text{CaO} \cdot \text{SiO}_2$ necessary for this condition to exist is of interest. Fig. 18a represents values of the ζ function for mixes in the binary system $\text{CaO} - C_2S$ at a given

* Free lime estimated by the method of LERCH and BOGUE, 'J. Ind. Eng. Chem.,' vol. 18 (7), p. 739 (1926).

temperature, assuming arbitrary values of ζ for CaO and C_2S . Points C', C, and C'' represent possible values of ζ for C_3S at this temperature. In the first case (C'), C_3S would be stable, in the last case (C'') unstable, while the ζ value corresponding to C would represent the transition condition $C_3S \rightleftharpoons CaO + C_2S$.*

If the value of ζ for C_2S at a temperature of t° is x and the value for CaO at the same temperature is $(x + y)$, the value of ζ for the transition condition of C_3S is

$$x + y \left(\frac{BC}{AB} \right) \text{ or } (x + 0.25y) \text{ approximately.}$$

Whenever ζ C_3S is less than $(x + 0.25y)$, the compound is stable.

Fig. 18b is a graph of hypothetical ζ values of CaO and C_2S with increasing temperature. The inflections in the C_2S curve correspond to the inversion points of the γ to β and β to α forms respectively. Points on the intermediate curve PQ are plotted 0.25 of the vertical distance between corresponding points on the CaO and C_2S curves, *i.e.*, the curve represents possible transition conditions for C_3S . If the curve for C_3S now has the form shown, the compound is only stable in that portion between R and S. In the figure

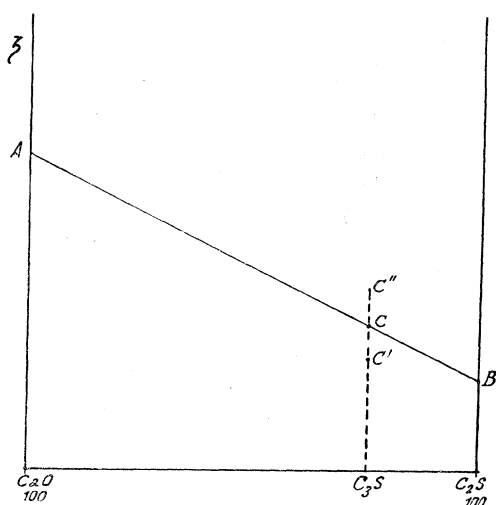


FIG. 18a

these points are shown as being at 1250° C and 1900° C respectively.

The changes in slope of the C_2S curve owing to the two inflections enhance the possibility of the existence of this type of limited stability of tricalcium silicate, yet it is quite possible to devise a similar region of stability for C_3S when the C_2S curve is continuous.

INVARIANT POINTS AND COURSES OF CRYSTALLIZATION

The system $C_2S-C_4AF-C_5A_3$ —This case presents no complexities, crystallization curves are of the simplest type and the final stage of crystallization for all mixes produces mixtures of the three components.

The system $CaO-C_2S-C_4AF$ —In discussing this system and the quaternary system, when C_3S appears in the finally crystallized mix, it is to be understood that this refers to the state above the decomposition temperature of 1250°. The system is divided into two regions by the composition line $C_3S - C_4AF$ (fig. 10a) and the products of final crystallization in each region are respectively CaO, C_3S , C_4AF , and C_3S , C_2S , C_4AF . The invariant point X lies in its own region, but the point W at which C_3S , C_2S , and C_4AF are in equilibrium lies outside of its corresponding region. It follows that there is no maximum on the C_3S-C_4AF boundary line and temperatures will rise along this line from the point X to W. The latter point is not therefore

* ALKEMADE, 'Z. phys. Chem.,' vol. 11, p. 289 (1893).

a eutectic, but a quintuple invariant point. Point X at which CaO , C_3S , and C_4AF are in equilibrium is a ternary eutectic in this system. The greater part of the area affords simple types of crystallization paths, but complications are introduced by the displacement of the C_3S field to the high lime side of the $\text{C}_3\text{S—C}_4\text{AF}$ line. There are in all 23 different crystallization courses in the system, but it is not considered necessary to outline them in detail since they can be readily obtained from the diagram (fig. 10a).

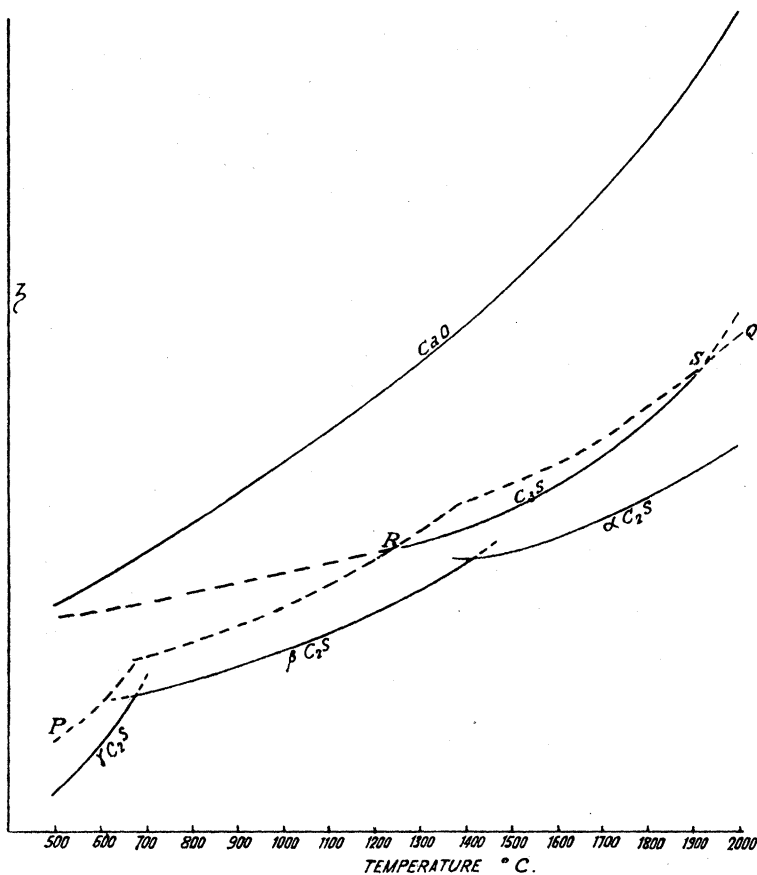


FIG. 18b

The quaternary system—The tetrahedron can be divided into three different regions, in any one of which the final products of crystallization are the same. These are defined by the bounding planes (see figs. 20 and 21, Plate 1) as follows:—

Region (i) ($\text{CaO—C}_4\text{AF—C}_3\text{S}$) ($\text{CaO—C}_4\text{AF—C}_3\text{A}$) ($\text{C}_3\text{A—C}_3\text{S—C}_4\text{AF}$)
($\text{CaO—C}_2\text{S—C}_3\text{A}$);

Region (ii) ($\text{C}_3\text{S—C}_3\text{A—C}_4\text{AF}$) ($\text{C}_3\text{S—C}_2\text{S—C}_3\text{A}$) ($\text{C}_3\text{S—C}_2\text{S—C}_4\text{AF}$)
($\text{C}_2\text{S—C}_3\text{A—C}_4\text{AF}$);

Region (iii) ($\text{C}_2\text{S—C}_3\text{A—C}_4\text{AF}$) ($\text{C}_3\text{A—C}_5\text{A}_3\text{—C}_4\text{AF}$) ($\text{C}_2\text{S—C}_3\text{A—C}_5\text{A}_3$)
($\text{C}_2\text{S—C}_4\text{AF—C}_5\text{A}_3$).

The final products of crystallization are :—

Region (i) CaO , C_3A , C_4AF , and C_3S .

Region (ii) C_3S , C_2S , C_3A , and C_4AF .

Region (iii) C_2S , C_3A , C_4AF , and C_3A_3 .

The invariant point T_1 lies outside the region in which the four components at equilibrium at T_1 are the final products of crystallization (*i.e.*, region (i)). This point cannot therefore be a eutectic and must be a sextuple invariant point in the system. This is illustrated by fig. 17*a* which shows, in exaggerated form, the C_3S boundary surface against C_3A and C_4AF and the trace of the plane $C_3S-C_4AF-C_3A$ across it. If the trace of the plane passed through the line $T_1 T_2$, the intersection would be a maximum temperature on $T_1 T_2$, but, in its actual position, temperatures must rise on $T_1 T_2$ towards the plane, *i.e.*, T_1 must be at a higher temperature than T_2 . Fig. 19 shows this similarly.

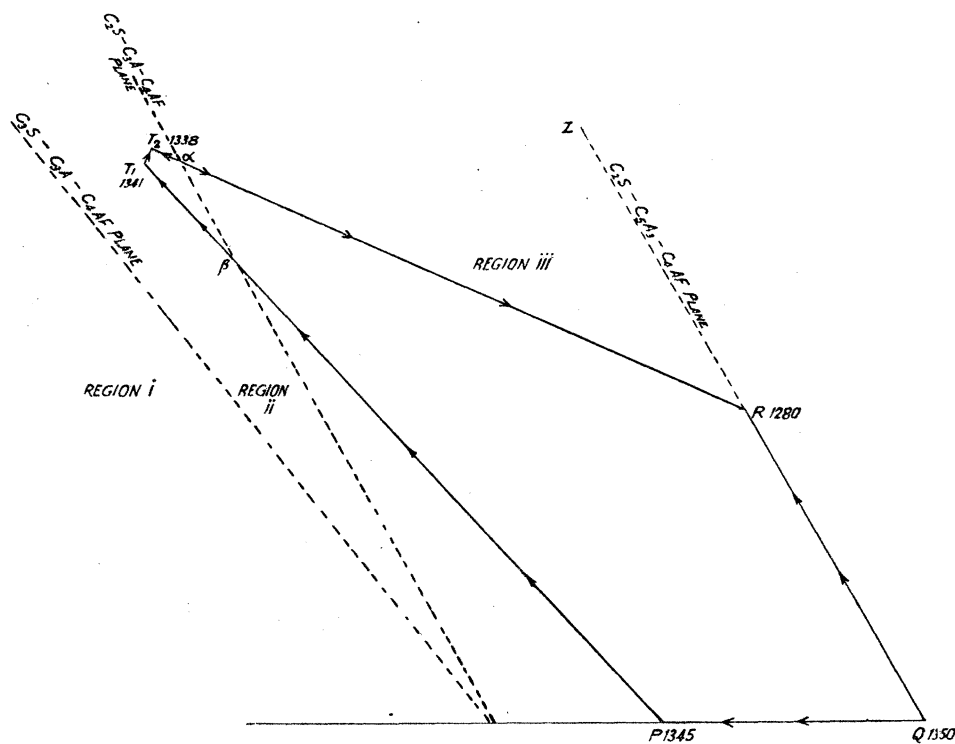


FIG. 19—Drawing of $C_3A - C_4AF$ surface. Showing trace of $C_2S - C_3A - C_4AF$ plane cutting T_2R and T_1Q at α and β respectively. Arrows show direction of falling temperature.

N.B.—Actually the surface does not lie in one plane (see fig. 20, Plate 1). The figure represents a projection on to the horizontal.

The $C_2S - C_3A - C_4AF$ plane is drawn slightly displaced to the right of its true position for illustration purposes.

For point T_2 to be a eutectic it should fall within region (ii). In fact, however, it may lie just within region (ii) or (iii). The composition given ($\text{CaO } 54.8\%$, Al_2O_3 22.7% , SiO_2 6.0% , Fe_2O_3 16.5%) is within region (ii) but the position is such

that if the point had the composition ($\text{CaO } 54.9\%$, Al_2O_3 23.1% , SiO_2 6.0% , Fe_2O_3 16.0%), which is within the experimental error of determination, the point would lie practically on the $C_2S\text{—}C_3A\text{—}C_4AF$ plane and a little lower iron content would bring it into region (iii). It is, therefore, not possible definitely to assess T_2 as a quaternary eutectic. If T_2 does fall in region (ii) and is a eutectic, the line T_2R , fig. 20, Plate 1, must show a maximum temperature where it is cut by the plane $C_2S\text{—}C_3A\text{—}C_4AF$ and the C_2S volume, the C_4AF volume and the $C_2S\text{—}C_4AF$ surface should show maximum temperatures along the $C_2S\text{—}C_3A\text{—}C_4AF$ plane. The line from the $C_2S\text{—}C_4AF$ eutectic (point V) to the maximum on T_2R should also be a maximum line in the $C_2S\text{—}C_4AF$ boundary surface. There will not be a maximum at the intersection of the $C_3A\text{—}C_2S\text{—}C_4AF$ plane on the line T_1P and hence, in the $C_3A\text{—}C_4AF$ boundary surface, a maximum must start from the maximum point in T_2R , run along the intersection of the plane with the $C_3A\text{—}C_4AF$ boundary surface but fade out before reaching the CaO side of the surface. Fig. 19, a horizontal projection of the $C_3A\text{—}C_4AF$ surface is of assistance in demonstrating this point.

If T_2 falls in region (iii) and is therefore not a eutectic, temperatures will fall continuously along T_2R and none of the above maxima will exist. Experimentally the maximum on T_2R cannot be detected as it is very close to the sextuple point T_2 , and the temperature gradients are small.

In a similar manner it is not possible to determine whether R is a eutectic or a sextuple point, since the experimental evidence shows the point to be on the $C_4AF\text{—}C_2S\text{—}C_5A_3$ surface, while the error allows it to be slightly to either side of this plane. For R to be a eutectic it must not lie outside region (iii) (*i.e.*, not to the right of line QZ, fig. 19).

The number of possible crystallization paths in the quaternary system is very large, some of them being of the simplest type while the majority are more complex. This variety and complexity of paths arises partly from the presence in the system of two compounds whose compositions fall outside their primary phase volumes, but it is much enhanced by the manner in which the C_3S primary phase volume lies first to one side, and then passes to the other side, of the $C_3S\text{—}C_3A\text{—}C_4AF$ plane. The crystallization region (i) includes the major part of the CaO primary volume and a portion of the C_3S and C_4AF volumes. The C_3A primary volume does not appear in it at all though this compound is present in the final crystallization of all mixes. The crystallization region (ii), in general, contains the most complex crystallization paths in the model. While C_3A appears in the products of final crystallization, it is only present, as a primary phase, in a very small region near T_1 . The primary volume of CaO appears, though this compound is not present in the final stages of crystallization, the volume of C_3S crosses the region and part of the volumes of C_2S and C_4AF lie within it. The crystallization region (iii) is perhaps the simplest of the three. All the compounds of final crystallization are present as primary volumes, but in addition, the volumes of both CaO and C_3S extend into it.

It is not possible within the limits of space available to outline all the crystallization paths, or even to discuss each different type which arises, but examples of some of the more important types may be given.

Crystallization path with no disappearing phases—Points in the primary volume of C_2S , lying in region (iii), chosen such that a line produced from C_2S through the particular composition will meet the C_2S — C_4AF boundary surface ($WVRT_2$), will have phases appearing in the following order :— C_2S ; C_2S and C_4AF ; C_2S , C_4AF , and C_3A ; C_2S , C_4AF , C_3A , and C_5A_3 .

Crystallization paths involving disappearing phases—Compositions lying in regions (ii) and (iii) and whose primary phase is CaO all involve paths with disappearing phases and typical cases may be quoted from this zone.

(1) One phase disappears along a boundary surface and the crystallization path crosses another primary phase volume :

Part of the zone mentioned above can give rise to the following course :—CaO ; CaO and C_3S ; C_3S ; C_2S and C_3S ; C_2S , C_3S , and either C_3A or C_4AF ; C_2S , C_3S , C_3A , and C_4AF .

(2) One phase disappears along a quintuple line and the crystallization path crosses another boundary surface :

Another part of the same zone gives rise to the following :—CaO ; CaO and C_3S ; CaO, C_3S , and C_3A ; C_3S and C_3A ; C_3S , C_3A , and C_2S ; C_3S , C_3A , C_2S , and C_4AF .

(3) One phase disappears at a sextuple point and the crystallization path follows another quintuple line :

Another part of the same zone may crystallize in the order :—CaO ; CaO and C_3A ; CaO, C_3A , and C_3S ; CaO, C_3S , C_3A , and C_4AF at the sextuple point T_1 , where CaO redissolves in the liquid and the course continues :— C_3A , C_3S , and C_4AF ; C_3A , C_3S , C_4AF , and C_2S at T_2 .

All three types quoted are from compositions lying also in region (ii). To give a closer geometrical definition of the position of each quoted part in the zone is difficult, but it is a comparatively simple operation to work out paths for individual points, using the principles outlined earlier.

That part of the CaO primary volume in this zone which lies also in region (iii) gives rise to more complicated paths which are a combination of the types given above. Thus, if a point in the CaO primary volume in (iii) is chosen so that the line through CaO and the point meets the CaO— C_3S surface, there may arise the following path :—CaO ; CaO and C_3S ; C_3S ; C_3S and C_3A ; C_3S , C_3A , and C_2S ; C_3A and C_2S ; C_3A , C_2S , and C_5A_3 ; C_3A , C_2S , C_5A_3 , and C_4AF in which it may be seen that the first two phases to crystallize disappear before the final stage is reached.

Temperature contours—The addition of C_4AF to the ternary system CaO— C_2S — C_5A_3 has a marked effect in lowering the temperature gradients, particularly in the low lime, high iron regions. For example, there appears to be only about 10° C difference in temperature between the binary, ternary, and quaternary invariant points V, W, and T_2 . The effect points to a probable high degree of dissociation in the liquid phase in this part of the system.

The work described in this paper was carried out at the Building Research Station, and the authors wish to express their thanks to Dr. R. E. STRADLING and Mr. B. H. WILSDON for their continued interest and encouragement during the progress of this work.

SUMMARY

(1) The phase relations in the following systems have been determined :—

- (a) Binary system $C_2S\text{—}C_4AF$.
- (b) Ternary system $\text{CaO—}C_2S\text{—}C_4AF$.
- (c) Ternary system $C_2S\text{—}C_5A_3\text{—}C_4AF$.
- (d) Quaternary system $\text{CaO—}C_2S\text{—}C_5A_3\text{—}C_4AF$.

(2) No new compounds were observed in any of the systems. Table VII gives a summary of data on the invariant points.

TABLE VII

Invariant point	Composition %				Temperature °C
	CaO	Al_2O_3	SiO_2	Fe_2O_3	
Binary system $C_2S\text{—}C_4AF$: eutectic	49.6	17.1	6.5	26.8	1350 ± 10
Ternary system $C_2S\text{—}C_5A_3\text{—}C_4AF$: eutectic	50.0	34.5	5.6	9.9	1280 ± 5
Ternary system $\text{CaO—}C_2S\text{—}C_4AF$					
i eutectic of CaO, C_3S, C_4AF	52.8	16.2	5.6	25.4	1347 ± 5
ii Quintuple point of C_2S, C_3S, C_4AF	52.4	16.3	5.8	25.5	1348 ± 5
Quaternary system : invariant points					
i $\text{CaO}, C_3S, C_3A, C_4AF$	55.0	22.7	5.8	16.5	1341 ± 5
ii C_3S, C_2S, C_3A, C_4AF	54.8	22.7	6.0	16.5	1338 ± 3
iii $C_2S, C_3A, C_5A_3, C_4AF$	50.0	34.5	5.6	10.0	1280 ± 5

(3) Temperature relations and crystallization paths in quaternary systems are discussed with reference to, and examples from, the present investigation.

(4) The compound $3\text{CaO} \cdot \text{SiO}_2$ is unstable in this system below 1250°C and above 1900°C , giving the same decomposition products in either case. It is shown that the lower decomposition point is a definite temperature at which the whole of the compound is dissociated, although the actual rate of decomposition is very slow.

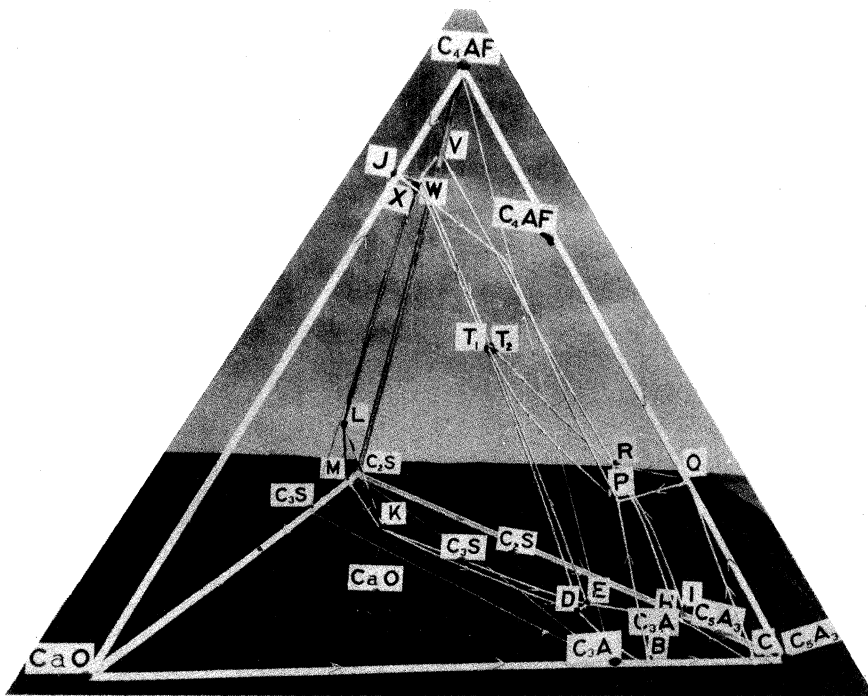


FIG. 20

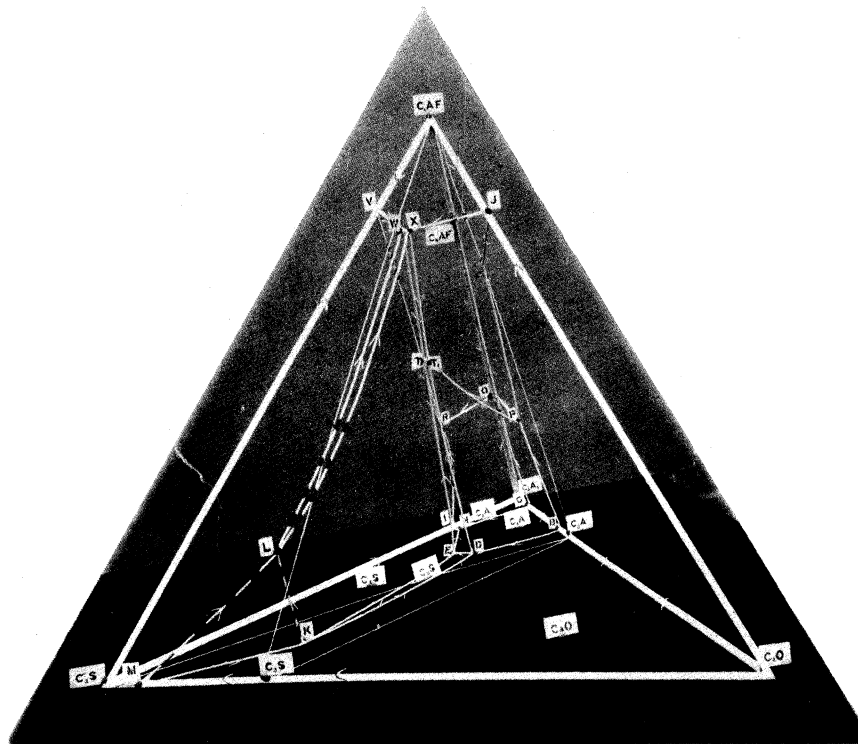


FIG. 21

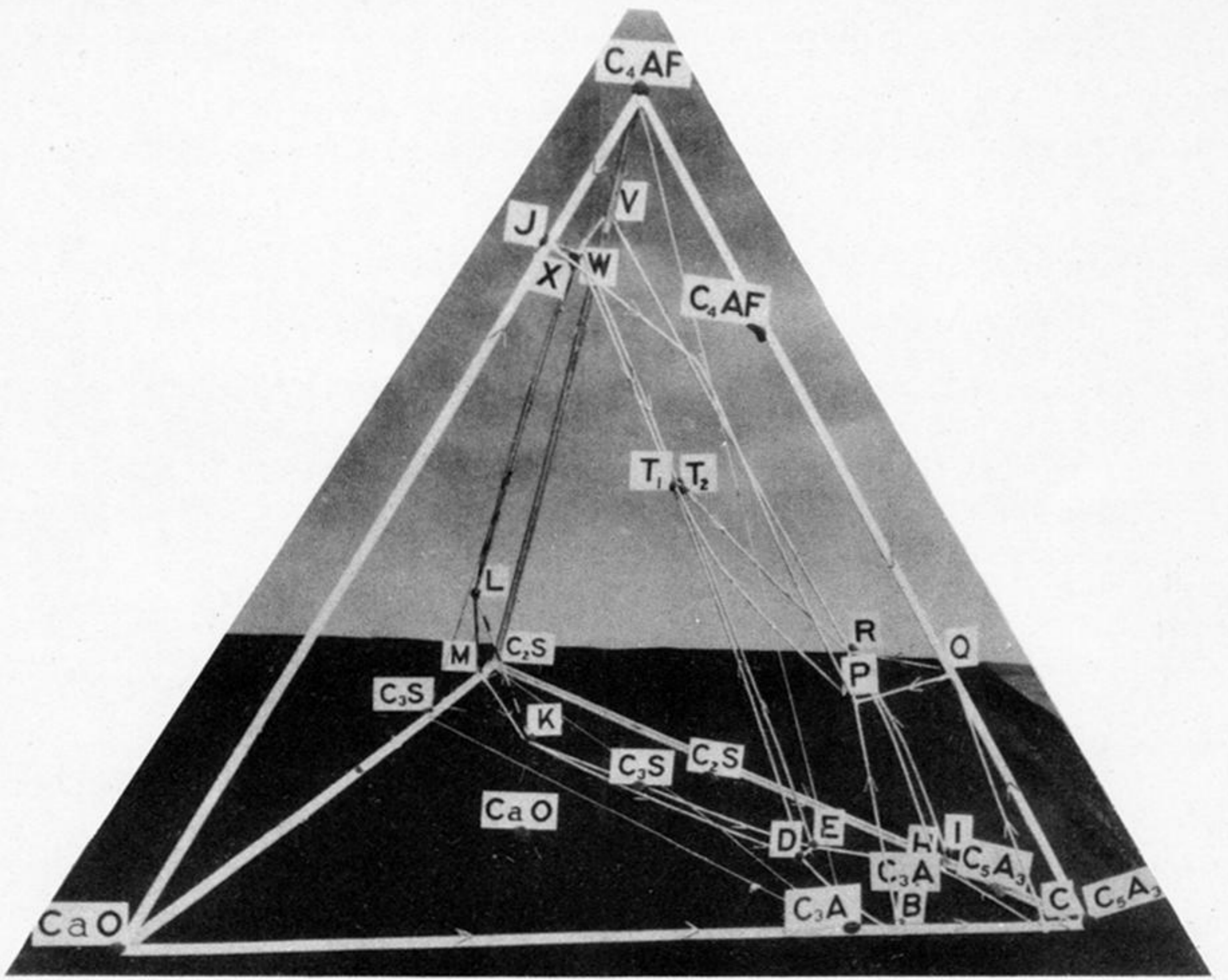


FIG. 20

Downloaded from rsta.royalsocietypublishing.org

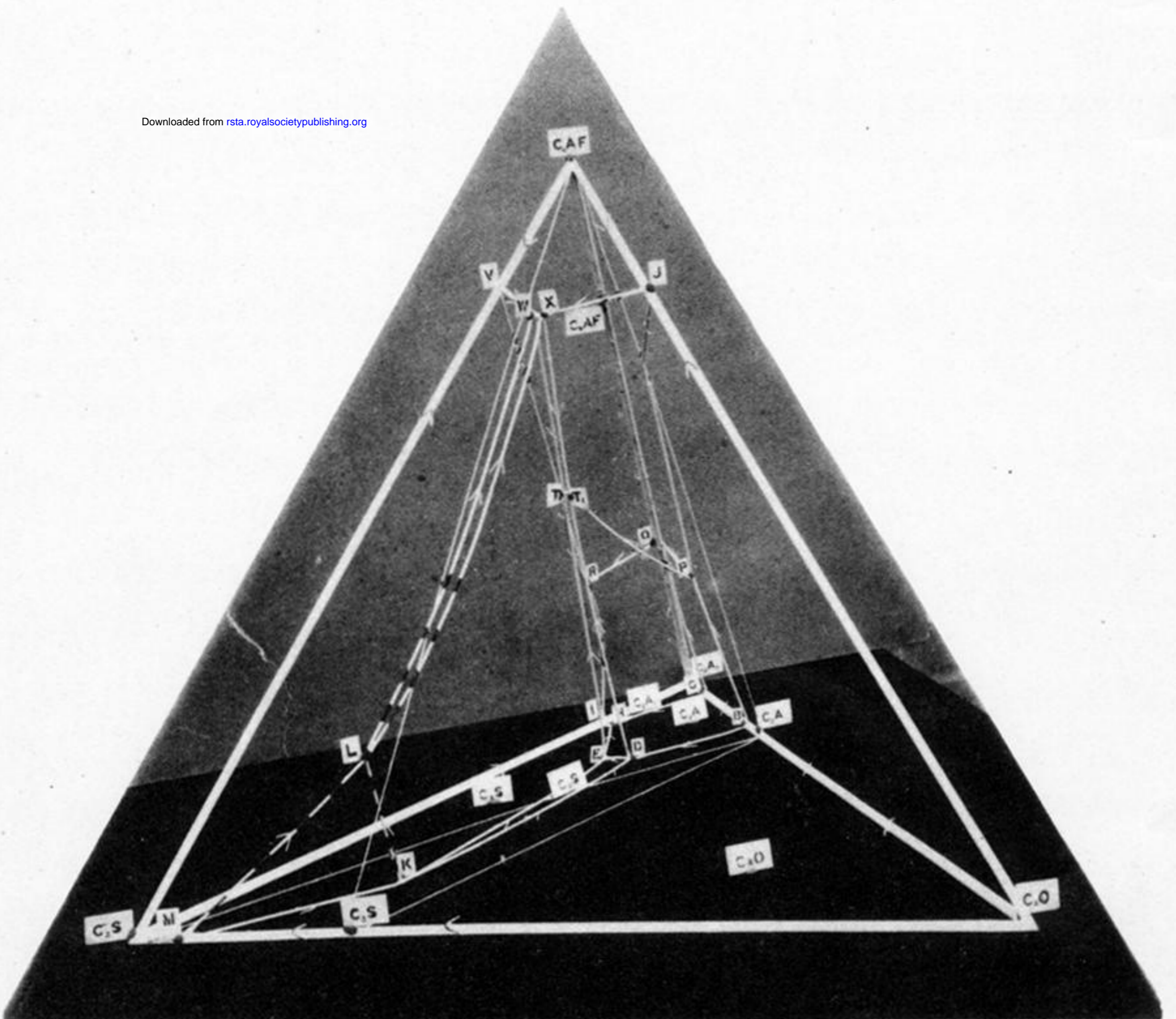


FIG. 21